Title

I. OPTICALLY DETECTED NUCLEAR QUADRIPOLE RESONANCE AND TRANSFERRED HYPERFINE COUPLING IN MOLECULAR CRYSTALS II. ELECTRON-ATOMIC HYDROGEN SCATTERING: TWO APPROACHES

Author

Yuen, David A.

Publication Date

1971-06-01

D. A. Yuen

UCRL-20702

c.2

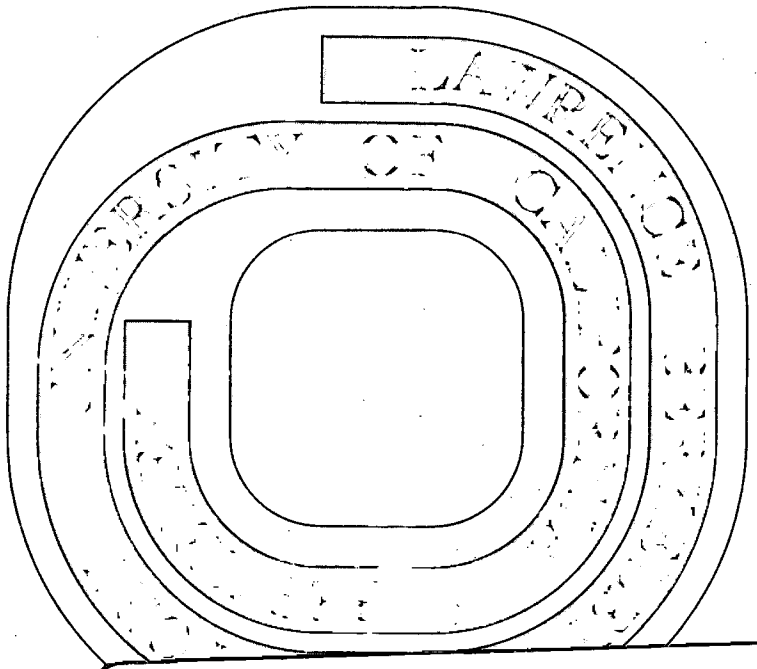

I. OPTICALLY DETECTED NUCLEAR QUADRUPOLE RESONANCE AND TRANSFERRED HYPERFINE COUPLING IN MOLECULAR CRYSTALS II. ELECTRON-ATOMIC HYDROGEN SCATTERING: TWO APPROACHES

David A. Yuen
(M. S. Thesis)

June 1971

AEC Contract No. W-7405-eng-48

34

DISCLAIMER

I. OPTICALLY DETECTED NUCLEAR QUADRUPOLE RESONANCE AND TRANSFERRED HYPERFINE COUPLING IN MOLECULAR CRYSTALS

II. ELECTRON-ATOMIC HYDROGEN SCATTERING: TWO APPROACHES

Contents

I. OPTICALLY DETECTED NUCLEAR QUADRUPOLE RESONANCE AND TRANSFERRED HYPERFINE COUPLING IN MOLECULAR CRYSTALS

II. ELECTRON-ATOMIC HYDROGEN SCATTERING: TWO APPROACHES

David A. Yuen

Inorganic Materials Research Division, Lawrence Radiation Laboratory
Department of Chemistry, University of California
Berkeley, California

ABSTRACT

I. The detection of the ground state nuclear quadrupole coupling constants of host molecules via the optically detected magnetic resonance (ODMR) of the triplet state of the guest is reported here. The two systems studied were the $^3\pi\pi^*$ state of quinoline doped in 1, 2, 4, 5 tetrachlorobenzene and the $^3n\pi^*$ state of pyrazine in 1, 4 dichlorobenzene.

II. The important atomic scattering system electron-hydrogen atom is studied by two approaches. For the medium high impact energy range, the distorted waves approximation, in the Eikonal guise, is developed. For low excitation energies the classical $\int$-matrix formalism is proposed for this very quantum-like system.

I. OPTICALLY DETECTED NUCLEAR QUADRUPOLE RESONANCE AND TRANSFERRED HYPERFINE COUPLING IN MOLECULAR CRYSTALS

A. Introduction

Recent optically detected zero field electron spin resonance experiments on $^3\pi\pi^*$ and $^3n\pi^*$[3] states of aza-aromatic compounds doped in molecular crystals have provided the triplet zero field parameters, nuclear-electron hyperfine interactions and the first measurement of the excited state ^{14}N and $^{35,37}Cl$ nuclear quadrupole coupling constants.[4,5] In the above experiments only intramolecular interactions have been considered. However, in molecular crystals the importance of intermolecular interactions is evident in the transfer of energy via excitons[6] and in the external heavy atom effect on phosphorescent radiative and radiationless decay,[7] to cite only two examples. It is therefore not surprising to expect the triplet wave function of an optically excited guest molecule to overlap the ground state wave function of the adjacent host molecules in doped molecular crystals and thereby transfer a small but finite spin density to the host. This phenomenon, which we will refer to as transferred hyperfine, has in fact been observed in the proton ENDOR of organic triplets by Hutchinson, et al.[8] and in carbon-13 and deuteron ENDOR by Kwiram et al.[9] We wish to report here positive evidence[10] for transferred hyperfine to ^{35}Cl and ^{37}Cl nuclei and an additional phenomenon which results from guest to host transferred hyperfine, specifically the detection of the ground state nuclear quadrupole coupling constants of the host molecules via the optically detected magnetic resonance (ODMR) of the triplet state of the guest. The two systems studied were the $^3\pi\pi^*$ state of quinoline doped in 1, 2, 4, 5 tetrachlorobenzene and the $^3n\pi^*$ state of pyrazine[3] in 1,4 dichlorobenzene.

B. Experimental Section

Next we shall give a brief description of the experimental equipment and procedures for the ESR experiment.[11] The basic experimental set-up is shown in Fig. 1.[11] The sample is mounted inside a helical slow wave structure which is attached to a rigid stainless steel coaxial-line suspended in a liquid helium dewar. A PEK 100-watt mercury short-arc lamp is used as the radiation source. To filter off high frequency components a combination of Corning glass and solution filters[12] were placed at the output of the lamp. As it is shown in Fig. 1, the phosphorescent radiation is collected at a right angle to the excitation source and focused through an appropriate Corning filter in order to remove the scattered radiation and finally is gathered onto the entrance slit of a Jarrel-Ash model 48-490, 3/4 meter Jarrel-Ash spectrometer. The emergent light signal is detected with an EMI 9558QB photomultiplier. The output of the photomultiplier is connected to a Keithley model 610CR electrometer through an adjustable load resistor; the cathode of the photomultiplier is maintained at -1800V by a Fluke 415 B power supply. Then the output from the electrometer is connected to a PAR model HR-8 lock-in amplifier. The output of the lock-in amplifier is connected to the y axis of a Hewlett-Packard model F035B recorder; the ramp voltage from the microwave sweep oscillator drives the x axis. A Hewlett-Packard sweep oscillator model 8690B equipped with plug-in units from the range of 0.1 to 18 GHz is employed for the microwave field. The microwave radiation is monitored through a directional coupler, and band-pass filter, and an isolator to the rigid co-axial line where the microwave helix is mounted. For signal-detecting purposes the microwave sweep oxcillator can be amplitude modulated with a Hewlett-Packard model 211 AR square wave generator, which is also connected to the

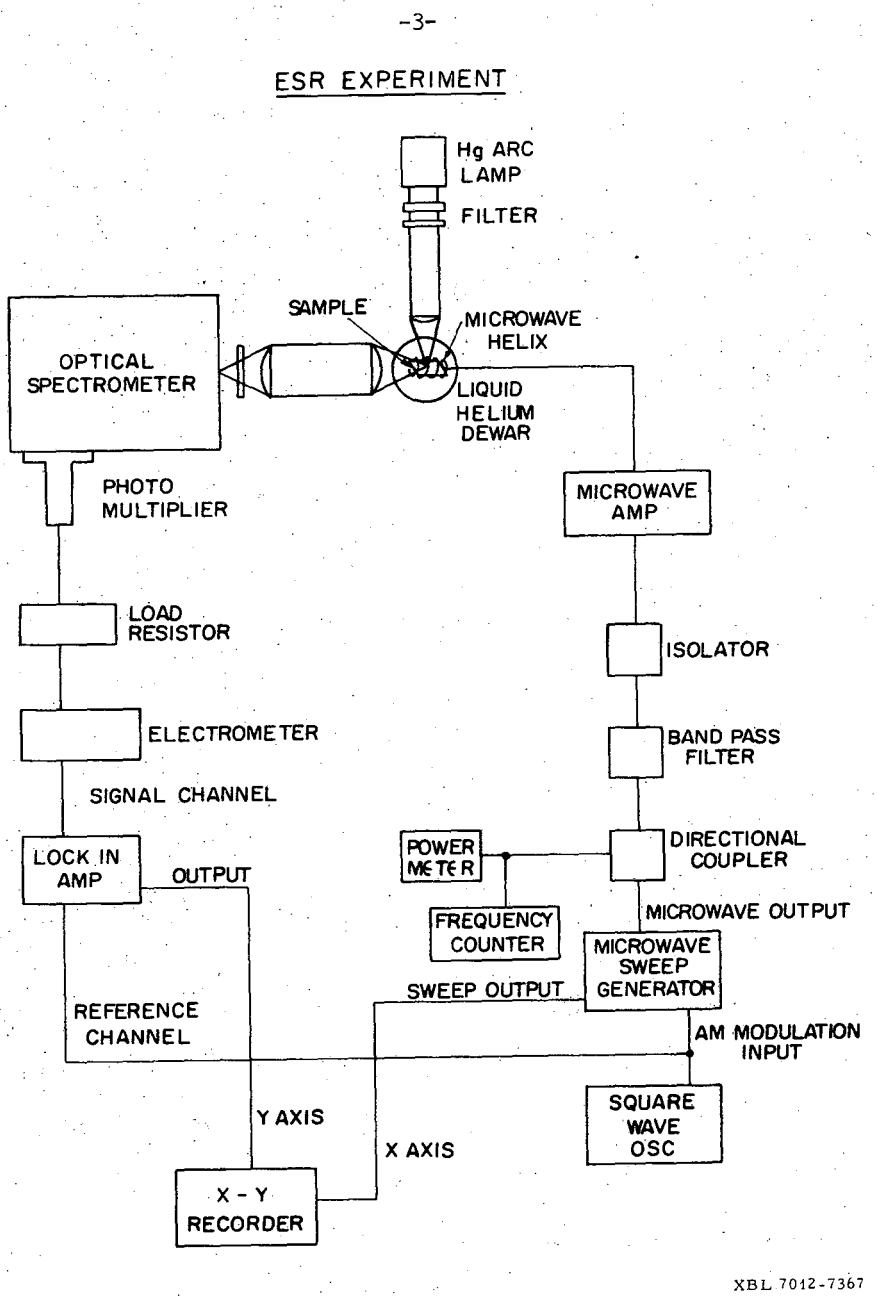

Fig. 1. Experimental arrangement for optically detected electron spin resonance in zero magnetic field.

reference channel of the lock-in amplifier. The helium dewar can be pumped to 1.75°K below the λ point, to avoid bubbling, with a Kinney model KTC-21 vacuum pump. The zero field ESR experiment then is conducted by observing the change in the phosphorescence of the sample while sweeping the appropriate microwave region.

C. Basic Development of the Triplet-State Hamiltonian

Since we are operating under the condition of zero external magnetic field, the complete quantum mechanical Hamiltonian[13] needed to describe the ODMR spectra can be formulated as follows.

$$H = H_{SS} + H_Q + H_{HF} \tag{1}$$

where H_{SS} represents the spin-spin interaction between the two unpaired spins, H_Q is the electric quadrupole interaction between the nuclear quadrupole moment and the field gradient of the external charge distribution at the nucleus, and H_{HF} the magnetic hyperfine interaction between the nuclear spin and net electron spin. It is interesting to see, that, by virtue of the electro- and magneto-static natures of the interactions, all of the above three Hamiltonians can be written in dyadic or tensorial notation and hence can be diagonalized. A brief review is given below to describe the explicit form of each term of the Hamiltonian and the resulting eigenvalue relationships.

H_{SS} is primarily the magnetic dipole-dipole interaction between the unpaired electrons in the excited triplet state; the spin-orbit coupling contribution in the zero field splitting has been calculated[29] to be small in value and hence can be neglected.

Transcribing the classical interaction between two magnetic moments into the quantum mechanical language,[13] we have then

$$H_{SS} = g_e^2 \beta_e^2 \frac{\underset{\sim}{S}_1 \cdot \underset{\sim}{S}_2}{r^3} - \frac{3(\underset{\sim}{S}_1 \cdot \underset{\sim}{r})(\underset{\sim}{S}_2 \cdot \underset{\sim}{r})}{r^5} \tag{2}$$

where ge is the anomalous electron g factor, which has been found to be basically isotropic for aromatic triplet states and to equal to the free electron value of 2.00232, β_e is the electron Bohr magneton, $e\hbar/2M_ec$. In tensorial notation, we have

$$H_{SS} = \underset{\sim}{S} \cdot \underset{\approx}{D} \cdot \underset{\sim}{S} \tag{3}$$

where $\underset{\approx}{D}$ is a real symmetric tensor and whose nine elements are given by

$$D_{xx} = \frac{1}{2} g_e^2 \beta^2 \frac{r^2 - 3x^2}{r^5}, \quad D_{xy} = \frac{1}{2} g_e^2 \beta^2 \frac{-3xy}{r^5} \tag{4}$$

and so forth, where we have assumed that the two electrons are fixed in space and the average then is taken over the triplet state electronic wave-function.[14] The Hamiltonian H_{SS} can be readily diagonalized in a principal axis system. The diagonalized form H'_{SS} is:

$$H'_{SS} = -X S_x^2 - Y S_y^2 - Z S_z^2 \tag{5}$$

where $-X = D_{xx}$, $-Y = D_{yy}$, and $-Z = D_{zz}$ are evaluated in the new principal axis system. Using LaPlace's equation as a constraint, in conventional ESR usage the Hamiltonian can be written as

$$H_{SS} = D(S_z^2 - \frac{1}{3} S^2) + E(S_x^2 - S_y^2) \tag{6}$$

where the famous D and E parameters are prescribed as:

$$D = \frac{3}{4} g_e^2 \beta_e^2 \frac{r^2 - 3z^2}{r^5}$$

$$E = \frac{1}{4} g_e^2 \beta_e^2 \frac{3y^2 - 3x^2}{r^5} \tag{7}$$

But as we all know $S^2 = 2$ for the triplet state, so finally in a neat form:

$$H_{SS} = D(Sz^2 - \frac{2}{3}) + E(Sx^2 - Sy^2). \tag{8}$$

Next we shall treat the electric-quadrupole interaction. From the Wigner-Eckart theorem,[16] a nucleus with spin greater than or equal to one has a non-vanishing electric quadrupole moment. From basic electrostatics, then there is an electrostatic interaction between the orientation of this quadrupole moment relative to the electric field gradient due to external charge distribution, which in the case of a free molecule arises principally from non-S electrons. To convert the classical electrostatic Hamiltonian to a quantum-mechanical one, one invokes the Wigner-Eckart theorem again, and uses the Racah coefficients[16] to evaluate the coefficients of the reduced matrix element of the quadrupole interaction, one can show that the following expression (using the tables in Condon and Shortley[17]) can be obtained

$$H_Q = \frac{eQ}{6I(2I-1)} \sum_{\alpha,\beta} V_{\alpha,\beta} \left[\frac{3}{2} I_\alpha I_\beta + I_\beta I_\alpha - \delta_{\alpha\beta} I^2\right] \tag{9}$$

where

$$Q = \sqrt{\frac{16\pi}{5}} \int \rho(r_n)\, r_n^2 Y_o^2(\Omega)\, d^3 r_n$$

the nuclear quadrupole moment, $(\text{length})^2$, α and β = (X, Y, Z), I is the nuclear spin quantum number, and $V_{\alpha,\beta} = \frac{\partial^2 V}{\partial\alpha\partial\beta}$.

Since H_Q is a symmetric tensor, one can express the Hamiltonian in terms of the axis system which diagonalizes the quadrupole tensor

$$H_Q = \frac{e^2 qQ}{4I(2I-1)} \left[(3I_z^2 - I^2) + \eta(I_x^2 - I_y^2)\right] \tag{10}$$

where $eq = \frac{\partial^2 V}{\partial z^2} = V_{z,z}$ or $\eta = \frac{V_{x,x} - V_{y,y}}{V_{z,z}}$ is the usual asymmetry parameter in NQR spectroscopy.[18]

Finally, one can use LaPlace's equation, $\sum_\alpha V_{\alpha,\alpha} = 0$, to reduce H_Q

to:

$$H_Q = \sum_{i=1}^{3} \varepsilon_i I_i^2, \text{ where } \varepsilon_i = \frac{3eQV_{i,i}}{6(2I-1)I} \tag{11}$$

which appears in the same canonical form as the zero-field Hamiltonian, H_{SS}. It is noteworthy to point out that the $V_{i,i}$ are the principal values of the quadrupole tensor.

Since the magnetic-dipole moment is an axial vector, a permanent magnetic dipole exists in nuclei with spin $\geq \frac{1}{2}$. The interaction of the nuclear magnetic moment with the electron magnetic moment, from classical E & M, leads to both anisotropic dipole-dipole interaction and the Fermi contact interaction.[14] The dipole-dipole interaction[14] between the nuclear moment and the electronic spin may be expressed as:

$$H_{HF}^{DD} = g_e\beta_e g_n\beta_n \frac{\underline{I} \cdot \underline{S}}{r^3} - \frac{3(\underline{I} \cdot \underline{r})(\underline{S} \cdot \underline{r})}{r^5} \tag{12}$$

where g_n is the nuclear g factor, and β_n is the nuclear Bohr magneton.

The above Hamiltonian can be written in dyadic form as before for the zero-field and quadrupole cases. In fact $H_{HF}^{DD} = \underline{S} \cdot \underline{\underline{A}} \cdot \underline{I}$ may be expanded as before. The $\underline{\underline{A}}$ matrix is symmetric and therefore, in its principal axis system, may be written as

$$H_{HF}^{DD} = A_{xx}S_xI_x + A_{yy}S_yI_y + A_{zz}S_zI_z \tag{13}$$

where

$$A_{ii} = -g_e g_n \beta_e \beta_n \frac{r^2 - 3\alpha^2}{r^5} + C$$

where

$$\alpha = (x,y,z)$$

and

$$C = \frac{8\pi}{3}\gamma_e\gamma_n\hbar^2 |\psi(0)|^2,$$

the Fermi contact term treated simple here as an additive constant; $|\psi(0)|^2$ is the electron density at the nucleus, ψ having a S orbital-like

symmetry; γ_i are the conventional gyromagnetic ratios.

D. Hamiltonian for Quinoline, the Model Case for Triplet State

Since we used quinoline as the guest molecule for both of our experiments, it would behoove us to work out the complete Hamiltonian for this molecule subjected to the zero-field experimental condition.

To be realistic and simplistic in our model we shall state the assumptions[11,19] made and the reasons for them:

(1) The principal axes of H_{SS}, H_Q, H_{HF} are coincident with the molecular axes.

(2) To first order only the out of plane component of the hyperfine Hamiltonian is taken into account.

(3) Since the Bohr magneton of the proton is 1836 times smaller than that for a free electron, the hyperfine interaction due to them can be considered as a second order interaction and has a magnitude less than 0.1 MHz.

Assumption (1) is justifiable on the grounds that since the nitrogen lone pair orbital lies on the z axis, then one of the principal axes of H_Q would be in this direction. From ESR spectra Maki[20] found that the nitrogen lone pair direction and the z axis were within a few degrees apart.

Assumption (2) can be justified by single crystal ESR measurements on quinoline by Vincent and Maki[20] where $A_{xx} >> A_{yy}$, A_{zz} for the nitrogen hyperfine interaction. The spin Hamiltonian for the quinoline molecule may be written for the axis system depicted in Fig. 2[11] as

$$H = X S_x^2 - Y S_y^2 - Z S_z^2 + \varepsilon_x I_x^2 + \varepsilon_y I_y^2 + \varepsilon_z I_z^2 + A_{xx} S_x I_x \tag{14}$$

which can be decomposed into two parts

$$H = H_0 + H_1 \tag{15}$$

where

$$H_0 = \sum_{i=1}^{3} - X_i S_i^2 + \sum_{i=1}^{3} \epsilon_i I_i^2 = H_{SS} + H_Q \qquad (16)$$

$$H_1 = A_{xx} S_x I_x$$

We shall use for our basis states the product functions $|\alpha\beta\rangle = \alpha_\mu \beta_2$, which are the eigenfunctions that diagonalize H_{SS} and H_Q. α,β refer to the electron and nuclear spin functions respectively; $\mu = (X,Y,Z)$ and $\nu = (x,y,z)$.

The effect of the various operators, S_i^2, I_i^2 can be easily found from the usual angular momentum operator relationships.[11,19] In this way $H_0 = H_{SS} + H_Q$ is readily obtained and H_{HF} is then treated as a first-order perturbation; terms $A_{yy} I_y S_y$, etc. are second order in nature. The complete Hamiltonian is then a 9×9 matrix as shown in Fig. 2, where the in-plane hyperfine elements, though negligibly small, have been included. The eigenvalues for this matrix, within our out-of-plane hyperfine perturbative approximation can be solved trivially via diagonalizing only 2×2 matrices. The results, from 2nd order perturbation theory are shown in Fig. 3.[11] From the center of gravity rule in perturbation theory, the energy of the states $|Zz\rangle$ and $|Zy\rangle$ are shifted by an amount β, where $\beta = \frac{A_{xx}^2}{Y-Z}$, while the states $|Yz\rangle$ and $|Yy\rangle$ are shifted by an amount $-\beta$, which is to be expected. Since $A_{xx} \simeq 20$ MHz, and $Y\text{-}Z_1 \cong 1000$ MHz we can make the approximation

$$\left|\frac{1}{Z+z-(Y-y)}\right| \sim \left|\frac{1}{Z-y}\right|$$

and

$$\left|\frac{1}{Z+y-(Y+z)}\right| \sim \left|\frac{1}{Z-y}\right| .$$

For the spin states which are coupled by the A_{xx} component we have then the following results summarized below in Table I:

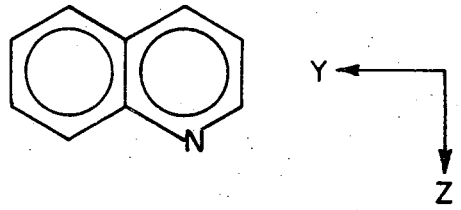

XX	XY	XZ	YX	YY	YZ	ZX	ZY	ZZ
X+x				-Azz				-Ayy
	X+y		Azz					
		X+z				Ayy		
	Azz		Y+x					
-Azz				Y+y				-Axx
					Y+z		Axx	
		Ayy				Z+x		
					Axx		Z+y	
-Ayy				-Axx				Z+z

XBL 7012-7270

Fig. 2. Hamiltonian matrix for triplet plus one I = 1 nuclear spin.

Table 1.

$\|Yy\rangle - \lambda\|Zz\rangle$	$\longleftarrow\!\!\!\!\!\!\!\!\longrightarrow$ $A_{xx}I_xS_x$	$\|Zz\rangle - \lambda\|Yy\rangle$
$\|Yy\rangle - \lambda\|Zy\rangle$	$\longleftarrow\!\!\!\!\!\!\!\!\longrightarrow$ $A_{xx}I_xS_x$	$\|Zy\rangle - \lambda\|Yy\rangle$

where

$$\lambda = \frac{A_{xx}}{Y-Z} \simeq 0.02$$

So the $|X\nu\rangle$ manifold in our approximation is left unaffected. Inclusion of other hyperfine terms would surely bring a myriad of other possible transitions.

E. Radiative Transitions and Relative Intensities

In this section we will consider the ODMR spectra when microwave radiation is applied to the sample. We shall see the importance of the hyperfine term, for it is the sole means of coupling the electron and nuclear-quadrupole Hamiltonians.

From time-dependent perturbation theory transitions between magnetic substates are caused by the magnetic dipole transition operator defined[13] by:

$$H_{RF}(r,t) = \underset{\sim}{A}(r)\cos(\omega t+\alpha) \cdot (\gamma_n \underset{\sim}{I} + \gamma_e \underset{\sim}{S}) \qquad (17)$$

where $\underset{\sim}{A}(r)$ is the spatial dependence of the magnetic field of the microwave radiation; α is some arbitrary phase angle; γ_n, γ_e are the nuclear and electron gyromagnetic ratios respectively.

From Fermi's Golden Rule[21] the intensity of the transition from one magnetic substate to another is:

$$I \propto |\alpha_{\mu_2}\beta_{\nu_2}|H_{RF}(r,t)|\alpha_{\mu_1}\beta_{\nu_1}|^2 \qquad (18)$$

Using the conventional angular momentum operator relationships, we

find the selection rules for the nuclear and electron spin transitions in the zero-field picture to be:

(1) The electron spin magnetic dipole operator, $H(r,t) \cdot (\gamma_e S)$, will induce transitions for states where $|\mu_2-\mu_1| = 1$, and $|\nu_2-\nu_1| = 0$.

(2) The nuclear spin magnetic dipole operator, $H(r,t) \cdot (\gamma_A I)$, will connect states for which $|\mu_2-\mu_1| = 0$, and $|\nu_2-\nu_1| = 1$.

From the fact that $\gamma e = \frac{\beta_e g_e}{\hbar} >> \gamma n = \frac{\beta_n g_n}{\hbar}$, a simple numerical calculation will show the following hierarchy for the relative intensities of the three possible kinds of transitions where

1. $|\mu_2-\mu_1| = 1$ and $|\nu_2-\nu_1| = 0$
2. $|\mu_2-\mu_1| = 0$ and $|\nu_2-\nu_1| = 1$
3. $|\mu_2-\mu_1| = 1$ and $|\nu_2-\nu_1| = 1$

Without the hyperfine perturbation, the respective relative intensities are: $I_1 \cong 10^6$, $I_2 \cong 10^2$, $I_3 \cong 0$.

Considering only the out-of-plane hyperfine component $A_{xx}I_xS_x$, we get the new relative intensities to be: $I_1' \cong 10^6$, $I_2' \cong 10^3$, $I_3' \cong 10^2$. It is important to note that the intensities can be described only in relative magnitudes, since there are competing rates of radiationless decay[22] to the T_0, triplet zero-field manifold, which render the population of the various levels to behave in a non-Boltzmann manner. It should be noted that it is necessary to have a hyperfine interaction in order to observe the nuclear quadrupole satellites, which arise from the first-order perturbed eigenfunction.

To confirm the assignment of the ODMR spectra and to improve on energy resolutions, electron nuclear double resonance (ENDOR)[15] experiments can be performed. (For a detailed description of the experimental procedures involved, the reader is encouraged to consult Mike Buckley's thesis.[11]) ENDOR transitions are shown in Fig. 3 as double arrows and

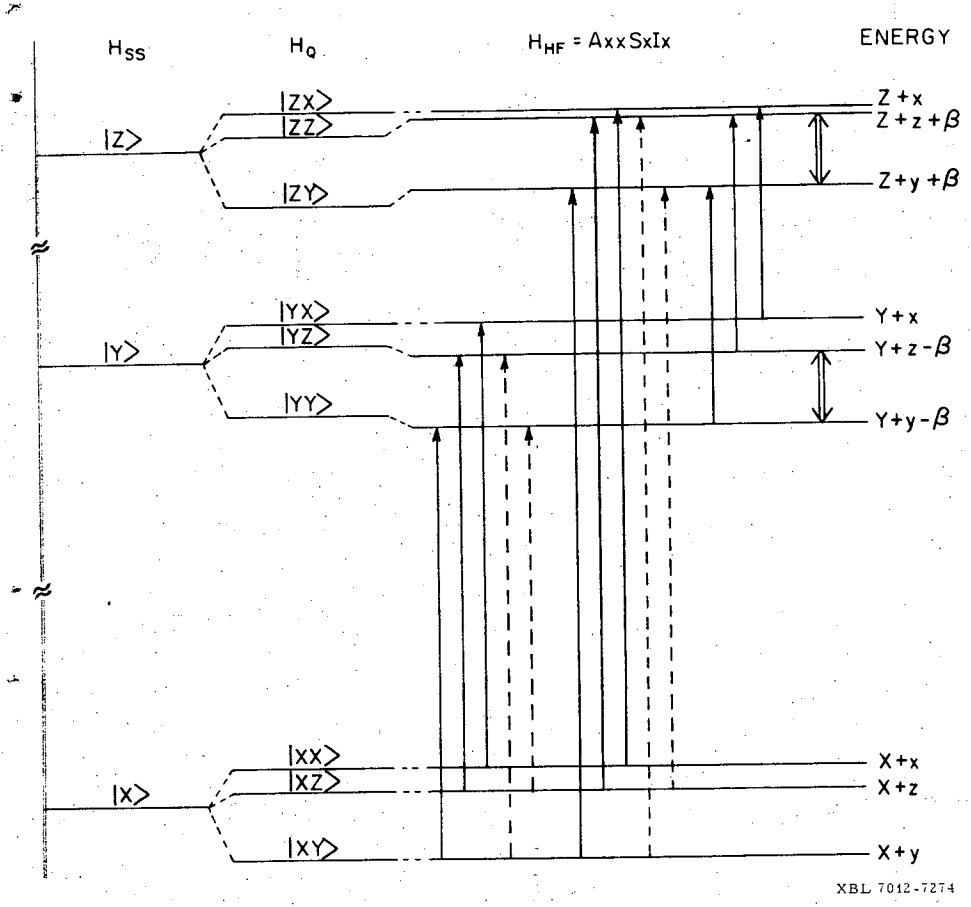

Fig. 3. Energy level diagram for the triplet and one I = 1 nuclear spin considering only the A_{xx} hyperfine component.

they correspond to transition of the type:

$$|Zy\rangle + \lambda|Yz\rangle \rightarrow |Zz\rangle \rightarrow \lambda|Yy\rangle$$

Proceeding in the proper usage of the magnetic dipole operator, as shown by Harris[5] et al., we have for the above transition the intensity as

$$I \propto 4\lambda^2\gamma_e^2 + 4\lambda\gamma_e\gamma_n + \gamma_n^2 \qquad (19)$$

There are then two types of ENDOR transitions possible in quinoline. We have in our laboratories observed an ENDOR transition[23] ~ 3.1 MHz while saturating the $Yz\rangle \rightarrow Zy\rangle$ satellite. (Data is from 10^{-3} M quinoline in Durene at 1.6°K in the 0-0 phosphorescent emission.)

We summarize all the transitions expected for the three zero-field transitions in terms of the components of the total Hamiltonian in Fig. 6.[11] It is obvious that the separation of the quadrupole satellites for the X → Z and Z → Y transitions is 2(z-y) and hence the nuclear quadrupole transition[18] $\frac{3}{4}$ eqQ($1-\frac{\eta}{3}$) is obtained. Theoretically the important physical quantities e^2qQ and η can be obtained independently provided other hyperfine tensor element are large enough to enable other ENDOR transitions to be observable. Lastly, the value of the hyperfine coupling constant A_{xx} can be trivially obtained from the separation of the two allowed components of each of the three transitions among the triplet manifold.

F. Guest-Host Interaction Phenomena

The above theoretical treatment agrees exceedingly well with the experimental data for quinoline in durene in the zero-field ESR framework. However, when 1,2,4,5 tetrachlorobenzene is used as a host, additional transitions, which cannot be explained using the above Hamiltonian, are observed. The same phenomenon was also observed for

pyrazine in paradichlorobenzene.

All materials were extensively purified and single crystals, 10^{-2}m quinoline and 10^{-3}m pyrazine in tetrachlorobenzene and paradichlorobenzene respectively were grown by Bridgeman refining techniques. Quinoline was detected using continuous wave techniques while pyrazine was detected using 20 Hz amplitude-modulation of the microwave field. All experiments were performed at 1.75°K while optically detecting the emission to the (0,0) state of the guest.

Figures 4[10] and 5[10] show the 2|E| and D + |E| zero field transitions[24] for quinoline and pyrazine respectively. The quinoline spectrum consists of a main peak at 1009.0 MHz flanked by a pair of satellites split symmetrically from the main peak by 37 MHz. The satellites are 13 MHz wide at half height and show some poorly resolved structure. The spectrum of pyrazine consists of a main peak at 9708.1 MHz and two pairs of symmetrical satellites split 27.0 MHz and 34.8 MHz from the center peak. Each has a width at half height of 7 MHz. The above results can be understood[19] in terms of intramolecular and intermolecular interactions.

The extraneous peaks suggest a chlorine/quadrupole interaction. If the overlap integral of the triplet state electronic eigenfunction and the eigenfunctions of the adjacent host molecules is non-zero then chlorine quadrupole and magnetic hyperfine interactions can take place. The Hamiltonian containing these additional interactions for the quinoline in tetrachlorobenzene system is

$$H = H_{SS} + H_Q^N + H_{HF}^N + H_Q^{Cl} + H_{HF}^{Cl} \qquad (20)$$

where H_{SS}, H_Q^N and H_{HF}^N have been given in a previous section, and

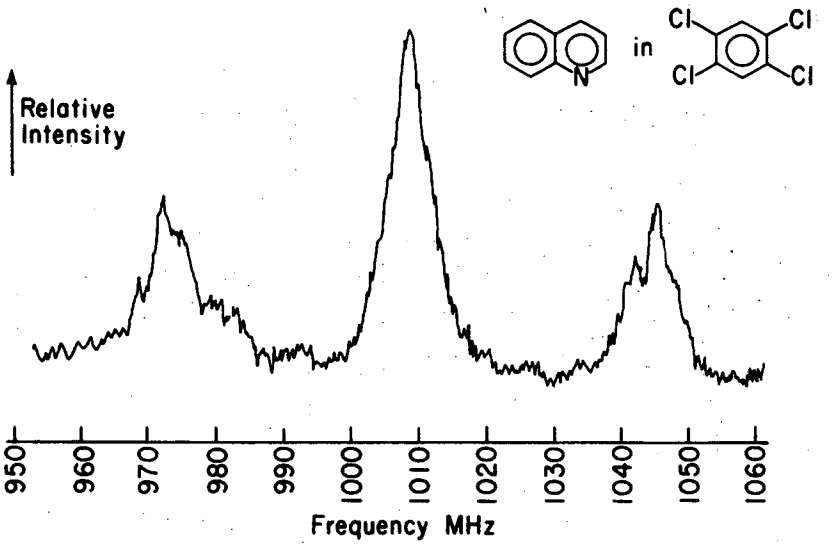

Fig. 4.

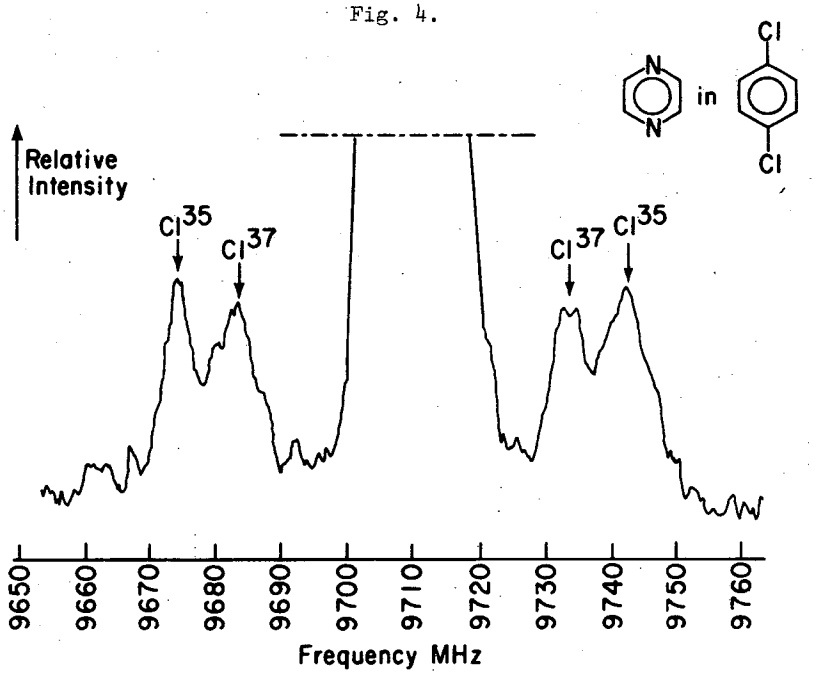

XBL 709-6566

Fig. 5.

Zero-field ESR spectra showing guest-host interaction.

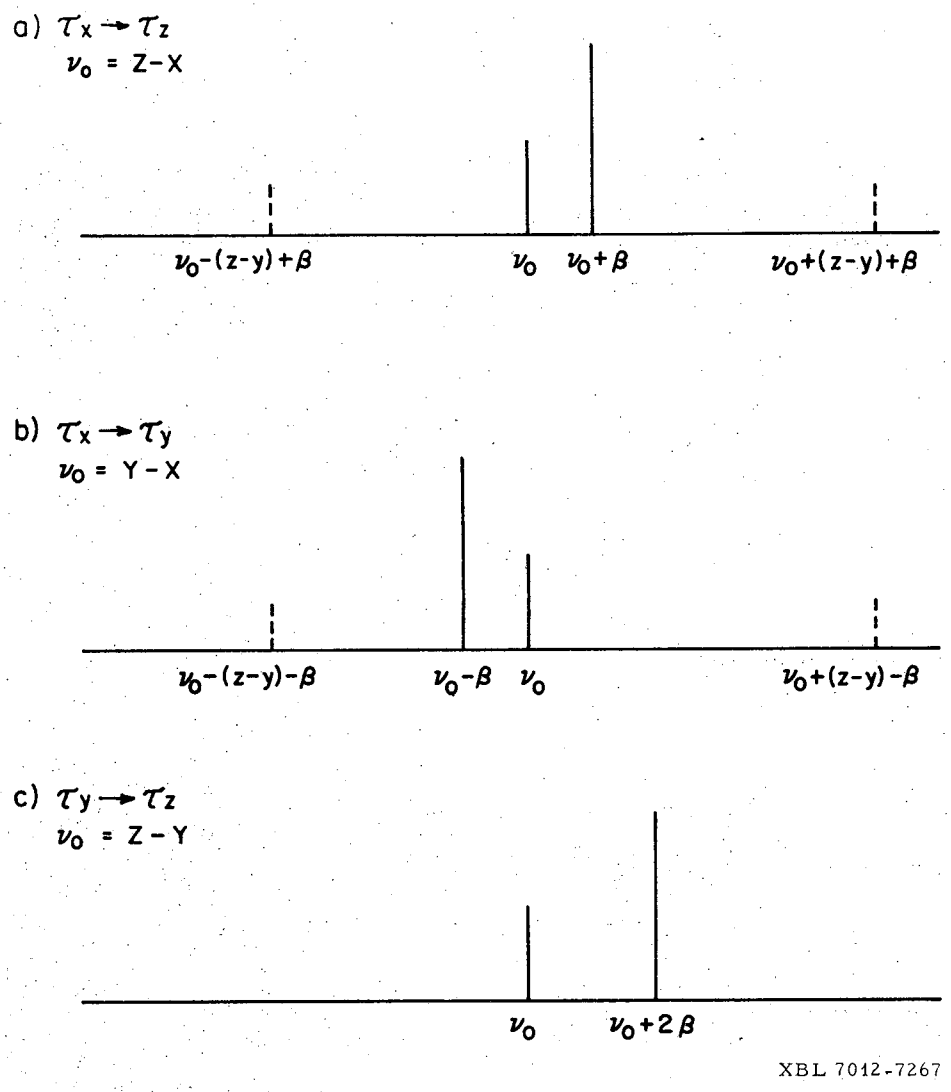

Fig. 6. ODMR spectra predicted for the energy level diagram shown in Fig. 3.

$$H_Q^{Cl} = \frac{eq^{Cl}Q^{Cl}}{12}\left[3m^2-\frac{15}{4}\right] + \frac{e^2q^{Cl}Q^{Cl}\eta}{24}\left[I_+^2-I_-^2\right] \qquad (21)$$

I_+, I_- are the standard raising and lowering operators, and

$$H_{HF}^{Cl} = A_{xx}^{Cl}\frac{1}{2i}\left(I_+S_x-I-S_x\right) \qquad (22)$$

Implicit in the above Hamiltonian are the following three assumptions:

(1) The interaction with only one chlorine nucleus need be considered;

(2) The principal axes of the chlorine quadrupole and hyperfine tensors coincide with the axis system for quinoline in durene employed by Buckley, Harris and Maki;[5]

(3) To first order, only one component of the chlorine hyperfine interaction, the out-of-plane component A_{xx}^{Cl}, need be included.

In regard to assumption (1), interaction of the resultant electron spins with more than one chlorine nuclear spin would make possible simultaneous electron spin and two chlorine spin transitions. This would produce wings split off from the center frequency by approximately twice the pure quadrupole frequency of the host. However they would probably be extremely weak, being second order in nature.

Assumption (2) is justified in that the use of a coincident axis system for the chlorine quadrupole and hyperfine interactions gave calculated results in agreement with the observed spectra, within experimental error. In fact Buckley,[11] in unpublished work, has rotated the axis system by as much as 15° and found that it would produce no observable effect on the spectrum.

Assumption (3) is made reasonable by noting that the major overlap of the π system of quinoline and surrounding host molecules is most likely to be perpendicular to the plane of the quinoline molecule.

From consideration of the states mixed by both H_{HF}^{N} and H_{HF}^{Cl}, four types of transitions between the electron spin manifolds can be classified using the magnetic dipole transition operator. These can be described as: (a) electron spin transitions, (b) simultaneous electron spin and nitrogen nuclear spin transitions, (c) simultaneous electron spin and chlorine nuclear spin transitions, and (d) simultaneous electron spin, nitrogen nuclear spin and chlorine nuclear spin transitions.

In terms of the above model, the 37 MHz wings observed in the spectrum of quinoline in 1,2,4,5-tetrachlorobenzene are accounted for as simultaneous electron spin and chlorine nuclear spin transitions. The width of these transitions is probably due to the presence of non-equivalent chlorine sites which broaden the Cl^{35} and Cl^{37} transitions to the extent that they all overlap, forming one broad peak.

Consider now the chlorine nuclear quadrupole and chlorine transferred hyperfine resulting from intermolecular interactions. In zero field the <u>first</u> order chlorine splittings of the host on the zero field transitions of the guest are independent of the orientation[13] of the host's principal field gradient tensor relative to the zero field tensor of the guest. Second order energy shifts of the chlorine satellites can occur but these are expected to be less than a few tenths of a MHz since they are dependent upon a very small transferred chlorine hyperfine interaction. If the chlorine asymmetry parameters are zero, the separation of chlorine satellites in Figs. 4 and 5 are simply the nuclear quadrupole coupling constants of the chlorine containing host molecules in the ground state. This is borne out by a comparison of the known ^{35}Cl nuclear quadrupole transitions for tetrachlorobenzene[25] (77°K, 36.8 and 36.9 MHz) and paradichlorobenzene[11,26] (77°K, 34.78 MHz, 4°K, 34.8 MHz). Thus it is important to stress that the chlorine

satellites acquire their intensity by transferred hyperfine. This then is positive evidence for such kinds of interaction. The most serious drawback of the method appears to be the line-widths of the chlorine satellites. In tetrachlorobenzene the line width probably results from multiple chlorine sites due to non-isomorphous[27] substitution of the guest and possibly from crystallographic twinning.[28] The spectrum of pyrazine in paradichlorobenzene exhibits narrower chlorine satellites to the extent that the ^{35}Cl and ^{37}Cl isotopic splittings are resolved. This is consistent with Kwiram's[3] low field optically detected ESR study which reports a two-site substitution of pyrazine in paradichlorobenzene.

In conclusion, we have here determined the ground state nuclear quadrupole coupling constant for the chlorine-containing host by observation of this transferred hyperfine coupling mechanism.

ACKNOWLEDGEMENTS

I wish to thank Mike Buckley for the use of his figures and other members of Chuck Harris's group, especially my buddies Mike Fayer and Bill Hughes.

REFERENCES

1. J. Schmidt and J. H. Van Der Waals, Chem. Phys. Letters 2, 640 (1968).
2. M. J. Buckley and C. B. Harris, Chem. Phys. Letters 5, 205 (1970).
3. L. Cheng and A. L. Kwiram, Chem. Phys. Letters 4, 457 (1969).
4. J. Schmidt and J. H. Van Der Waals, Chem. Phys. Letters 3, 546 (1969).
5. M. J. Buckley, C. B. Harris, and A. H. Maki, Chem. Phys. Letters 4, 591 (169).
6. A. S. Davydov, Molecular Excitons, New York: McGraw-Hill Book Company, 1962.
7. G. W. Robinson and R. P. Frosch, J. Chem. Phys. 38, 1187 (1963).
8. C. A. Hutchinson, Jr. and G. A. Pearson, J. Chem. Phys. 47, 520 (1967); C. A. Hutchinson, Jr. and B. E. Kohler, J. Chem. Phys. 51, 3327 (1969).
9. R. C. McCalley and A. L. Kwiram, Phys. Rev. Letters 24, 1279 (1970).
10. M. D. Fayer, C. B. Harris, D. A. Yuen, J. Chem. Phys. 53, 4719 (1970).
11. M. J. Buckley and C. B. Harris, Chem. Phys. Letters 5, 205 (1970); M. J. Buckley, Ph. D. Thesis, U. C. Berkeley (1971).
12. M. Kasha, J. Opt. Sci. Am. 38, 329 (1948).
13. A. Abragam, The Principles of Nuclear Magnetism, Oxford University Press, London, 1961.
14. C. P. Slichter, Principles of Magnetic Resonance, (Harper and Row, New York, 1963).
15. A. Carrington and A. D. McLachlan, Introduction to Magnetic Resonance, (Harper and Row, New York, 1967).
16. M. Tinkham, Group Theory and Quantum Mechanics, (McGraw-Hill Book Co., New York, 1964).

17. E. U. Condon and G. H. Shortley, The Theory of Atomic Spectra, (Cambridge U. P., 1967).
18. T. P. Das and E. L. Hahn, Nuclear Quadrupole Resonance Spectroscopy, (Academic Press, New York/London, 1958).
19. M. D. Fayer (Private Communication).
20. J. S. Vincent and A. H. Maki. J. Chem. Phys. 39, 3088 (1963).
21. K. Gottfried, Quantum Mechanics, Vol. I, (W. A. Benjamin Inc., New York, 1966).
22. R. S. Becker, Theory and Interpretation of Fluorescence and Phosphorescence (Wiley-Interscience, 1969).
23. M. D. Fayer, C. B. Harris, D. A. Yuen (unpublished data).
24. D and $|E|$ are the conventional ESR zerofield parameters.
25. P. Bray, J. Chem. Phys. 23, 220 (1955).
26. H. Meal, J. Am. Chem. Soc. 74, 6121 (1952).
27. E. T. Harrigan and N. Hirota, J. Chem. Phys. 49, 2301 (1968).
28. F. H. Herbstein, Acta. Cryst. 18, 997 (1965).
29. H. F. Hameka and L. J. Oosterhoff, Mol. Phys. 1, 358 (1958).

II. ELECTRON-ATOMIC HYDROGEN SCATTERING: TWO APPROACHES

A. Introduction

The excitation of atomic hydrogen[1] by electrons has received much more attention from research workers than has the excitation of any other atomic species, due to the relative simplicity of the system and the availability of accurate free-atom wavefunctions. The second half of this thesis will be directed toward this direction. Two approaches will be adopted: (1) the distorted waves approximation is developed for the mediumly high excitation energy range of between 50 and 150 electron volts (eV) (2) the recently innovated classical $\mathcal{S}$-matrix formalism[2] is employed for low impact energies below a Rydberg (13.6eV). The process 1s →2s, 2p are studied principally in each formalism. In both cases we shall state explicitly the limitations and validity of the physical approximations involved.

B. Historical Review of Some of the Approximation Schemes in Electron-Hydrogen Atom Scattering

In this section we shall briefly mention a few of the basic methods that have been employed for the e^--H problem.

The e^--H system is essentially a helium-like system whose Schrodinger wave equation is

$$\left[\frac{-\hbar^2}{2\mu}\nabla_1^2 - \frac{\hbar^2}{2m_e}\nabla_0^2 - \frac{e^2}{r_o} + \frac{e^2}{r_{o_1}} - \frac{e^2}{r_1}\right]\psi(r_Q,r_1) = E\psi(r_Q,r_1) \quad (1)$$

where μ is the reduced mass of the whole system and can be approximated by m_e, the mass of a free electron; r_Q, r_1 are arbitrarily chosen as the coordinates of the target and incident electrons, respectively. From now on we shall adopt the familiar atomic-unit system[(3)] where $m_e = \hbar = e = 1$.

The simplest, and good to first order for high energies and weak

potentials, is the first Born approximation,[1] the first iterated solution to the integral equation of wave-scattering solved with the Neumann series. The exchange amplitudes calculated in the plane-wave approximations are usually less satisfactory than the plane-wave direct amplitudes. The most common form of the plane-wave approximation to the exchange amplitude is the Born-Oppenheimer approximation. The exchange amplitude is considerably more difficult to evaluate than the direct amplitude because of the non-orthogonality of the two hydrogenic wavefunctions with different coordinate designation and the electron-electron interaction term. For the 1s→2s,2p excitations, closed analytical expressions for the exchange amplitude have been obtained by Corinaldesi and Trainor[5] using the Feynman parametrization technique.

Some other plane waves method that have been devised are higher-order Born approximations; Ochkur-Rudge[6] technique and a variant of the Born-Oppenheimer approximation employed by Bates,[7] Bassel, Gerjuoy,[7] and Mittleman.[7] For the 1s→2s,2p excitation problem very accurate calculations have been made by P. G. Burke and his cohorts.[8] In this approach the transmission matrix elements are obtained by means of the exact solution of the coupled integro-differential equations using numerical procedures; the order of the approximation depends upon the atomic states which are retained in the expansion of the total wavefunction, $\psi_{total}(r_Q,r_1)$. The anomaly-free variational technique on the electron-atom scattering problem has showed much promise by the recent calculations by R. K. Nesbet.[9]

Finally, the distorted wave technique has been used earlier by Erskine and Massey[10] and Ochkur[10] in the excitation of the 2s state of hydrogen. The distorted-waves method differs chiefly from the plane-waves theories insofar as it takes into account the distortion of both the incoming and outgoing waves by the static atomic potential. However,

the use of the second or higher order terms of the Born series makes partial allowance for this electronic distortion. From physical intuition, this distorted effect becomes more prominent as the relative kinetic-energy decreases. The formalism of the distorted-waves method is flexible in that it allows one to generate the approximate wavefunctions by whichever technique is best suited for the problem. Erskine and Massey obtained their distorted-waves by a variational method, while Ochkur calculated his partial waves by accurate numerical integration. Recent distorted-waves calculations by Shelton et al.[11] showed that they arrived at their distorted wavefunctions by numerically integrating outward the various partial waves in a static atomic potential. As we shall see, the distorted waves in our approach are invoked in the Eikonal spirit, since we are concerned with medium-high impact energies from 50 eV to 150 eV.

C. Transition Matrix Elements for Distorted Waves

In this section we shall give a brief formulation for the distorted waves treatment and the derivation of the transition matrix element in this physical picture. This is given in most standard references and we shall adhere to the notations in Messiah's book.[12]

$$\text{Let } H = H_i + V_i = H_f + V_f \tag{2}$$

where i, f denote the initial and final channels respectively and V is the total interaction potential

$$V_i = U_i + W_i,\ V_f = U_f + W_f \tag{3}$$

W_f, W_i are called the primary interactions; V_f, V_i are called the final and initial state interactions respectively.

Next we shall make the assumption that we know the eigenfunctions for the Hamiltonians

$$\bar{H}_i = H_i + V_i \text{ and } \bar{H}_f = H_f + V_f \tag{4}$$

So

$$\bar{H}_i X_i^{(\pm)} = E X_i^{(\pm)} \text{ and } \bar{H}_f X_f^{(\pm)} = E X_f^{(\pm)} \tag{5}$$

Distorting potentials U_i and U_f are suitably chosen so that the wavefunctions of $H_i + V_i$ and $H_f + V_f$ can be obtained exactly. $(\pm)$ notations represent the usual outgoing and incoming boundary conditions for the scattered waves. Hence W_i and W_f are the residual interactions in the initial and final channels.

The transition matrix can then be written in the Goldberger-Gell-Mann[13] two potential formula as

$$\begin{aligned} T_{f\leftarrow i} &= \langle \Phi_f | V_f - W_i | X_i^{(+)} \rangle + \langle \psi_f^{(-)} | W_i | X_i^{(+)} \rangle \\ &= \langle X_f^{(-)} | V_i - W_f | \Phi_i \rangle + \langle X_f^{(-)} | W_f | \psi_i^{(+)} \rangle \end{aligned} \tag{6}$$

where

$$\psi_i^{(+)} = \Phi_i + \frac{1}{E_i - H_i + i\varepsilon} V_i \psi_i^{(+)} \tag{7}$$

$$\psi_f^{(-)} = \Phi_f + \frac{1}{E_f - H_f + i\varepsilon} V_f \psi_f^{(-)} \tag{8}$$

are the respective Lippmann-Schwinger equations.[13] For the distorted waves apporach we make the approximations that $\psi_i^{(+)} \simeq X_i^{(+)}$, and $\psi_f^{(-)} \simeq X_f^{(-)}$ then

$$T_{f\leftarrow i}^{DW} = \langle X_f^{(-)} | V_i - W_i | \Phi_i \rangle + \langle X_f^{(-)} | W_f | X_i^{(+)} \rangle \tag{9}$$

for a system A+B → C+D, the initial and final state interactions U_f, U_i can only generate elastic scattering, so for excitation processes

$$\langle X_f^{(-)} \left| \begin{matrix} V_i \\ V_f \end{matrix} \right| \Phi_i \rangle \cong 0 \tag{10}$$

Thus

$$T^{DW}_{f\leftarrow i} = \left\langle X_f^{(-)} \middle| \begin{matrix} W_i \\ W_f \end{matrix} \middle| X_i^{(+)} \right\rangle \tag{11}$$

For inelastic collisions.

It is interesting to compare with the ordinary Born approximation where

$$T^{B}_{f\leftarrow i} \simeq \left\langle \Phi_f \middle| \begin{matrix} V_f \\ V_i \end{matrix} \middle| \Phi_i \right\rangle \tag{12}$$

The differential cross section is given by the expression

$$\sigma_{f\leftarrow i}(\theta) = \left| f_{f\leftarrow i}(\theta) \right|^2 \tag{13}$$

where $f_{f\leftarrow i}(\theta)$ is the scattering amplitude and is related by the usual way to $T_{f\leftarrow i}$, i.e.,

$$f_{f\leftarrow i}(\theta) = \left(\frac{K_f}{K_i}\right)^{1/2} \frac{1}{4\pi} T_{f\leftarrow i}(\theta) \tag{14}$$

Since the spins of the bound and free electrons are omitted, the differential cross-sections for the excitation processes are given by the familiar expression readily derivable from Fermi statistics:

$$\sigma_{f\leftarrow i}(\theta) = \frac{1}{4} \left| f_D(\theta) + f_E(\theta) \right|^2 + \frac{3}{4} \left| f_D(\theta) - f_E(\theta) \right|^2 \tag{15}$$

where $f_D(\theta)$ and $f_E(\theta)$ stand for the direct and exchange amplitudes respectively. For the 1S→2p process one just sum over the cross sections for the three magnetic substates:

$$\bar{\sigma}_{1s\rightarrow 2p} = \sum_{\mu=-1}^{+1} \sigma_{1s,2p\mu} \tag{16}$$

The following assumptions are made in regard to the formulation of the distorted Eikonal waves:

(1) The bound hydrogenic wavefunctions used in the Hartree field approximation are not distorted by the free electron. This is valid since the Eikonal approximation[14] is of an impulsive nature, in which the translational velocity is much greater than the internal velocities.

(2) The distorted wavefunction is written as a simple product of a bound hydrogenic wavefunction and a plane wave whose phase is perturbed by the Hartree field, but whose amplitude remains unchanged. For higher order Eikonal approximation the amplitude dependence can be properly accounted for.

(3) The z axis, in the Eikonal tradition, will be chosen as the direction of the oncoming electron.

(4) We shall make no correction to the curvature of the actual trajectory in the model; the trajectory is to be evaluated by a straight line. It should be noted that the Eikonal approximation covers a larger range of angles than for the Born approximation.[13]

In this way we can write our initial channel distorted wavefunction as

$$\tilde{X}_i^{(+)}(r_Q, r_1) = C\psi_{1s}(r_0) \exp\left(iK_Q \cdot r_1 - \frac{i}{2K_i} \int_{-\infty}^{z} V_i(b_1', z_1') dz_1' \right) \tag{17}$$

where C is an appropriate normalization constant; V_i is the asymptotic Hartree field experienced by the oncoming electron; b_1 is the initial impact parameter vector; z_1 is the incident direction vector; r_1 is the radial vector from the origin (in this case the proton) to the incident electron and is given by $r_1^2 = b_1^2 + z_1^2$. The hydrogenic wavefunctions used throughout are found in Pauling and Wilson,[15] pp. 132-139. In the same vein, for direct and exchange scattering the final channel distorted wavefunctions may be written as follows:

1. Direct scattering:

$$\tilde{X}_f^{(-)}(r_Q, r_1) = C\psi_n(r_0) \exp\left(iK_f \cdot r_1 - \frac{i}{2K_f} \int_{z_1}^{+\infty} U_f^I(b_1', z_1') d'z_1 \right) \tag{18}$$

(2) Exchange scattering:

$$\tilde{\chi}_f^{(-)}(r_Q, r_l) = C\psi_n(r_l) \exp\left(iK_f \cdot r_Q - \frac{1}{2K_f}\int_{z_0}^{+\infty} U_f^{II}(b_0', z_0')dz_0'\right) \tag{19}$$

where $\langle r_0|\psi_n\rangle, \langle r_l|\psi_n\rangle$ denote the final excited hydrogenic states (in our case, (2s and 2p); U_f^I, U_f^{II} are the final asymptotic Hartree potential felt by the emergent electron. The coordinate system used is shown in Fig. 1.

From Eq. (1) we see that the initial total Hamiltonian H can be partitioned into two parts $H = H_i + V_i$ where

$$H_i = -\frac{1}{2}(\nabla_l^2 + \nabla_0^2) - \frac{1}{r_0} \tag{20}$$

and

$$V_i = -\frac{1}{r_l} - \frac{1}{r_{0_l}}$$

The above quantum-mechanical Hamiltonian can be carried over exactly classically. This is done in the next part of the thesis, where the classical $\mathcal{S}$-matrix formulation of the same problem is explored.

For a reasonable approximation we shall use the Hartree potential[16] for our U_i and U_f the initial and final state interactions. The Hartree potential, being spherically symmetric, is especially suitable in view of the symmetry of the total Hamiltonian. Needless to say refinements can be built into the Hartree potential which take into account polarization effects. For atoms with more than one electron, electron correlations should be introduced in the total electronic wavefunction.

In general one calculates the spherically averaged Hartree potential U_i seen by each electron r_i by averaging the potential produced by the other bound electrons and the nucleus

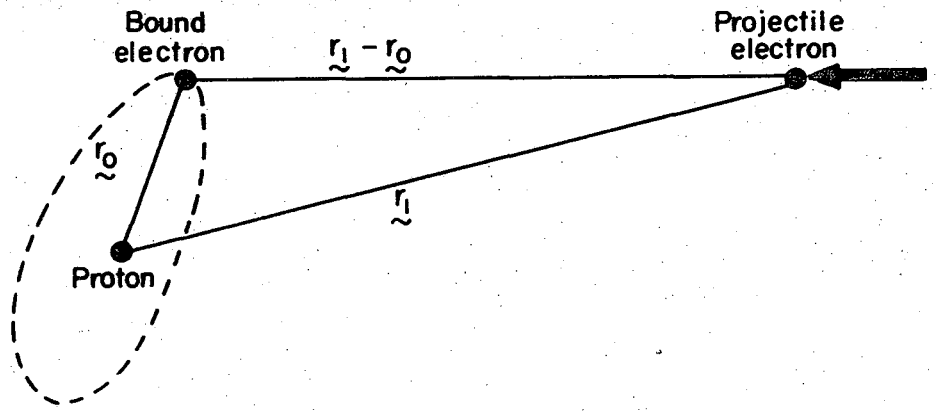

Fig. 1. Coordinate system for electron-atomic hydrogen system.

$$U_i(r_i) = -\frac{Z}{r_i} + \left\langle \sum_{j \neq i} \frac{1}{r_{ij}} \right\rangle \tag{21}$$

where Z is the atomic number.

The Hartree equations in matrix notation

$$\left[-\frac{\nabla_i^2}{2\mu} \underset{\approx}{1} + \underset{\approx}{U_i}(r_i) \right] \underset{\approx}{U_i} = \underset{\approx}{E_i}\, \underset{\approx}{U_i} \tag{22}$$

are coupled differential equations; μ the reduced mass. The solutions U_i are obtained by usual methods of numerical integration and <u>self-consistency</u> is used as a criterion. The $\tilde{X}_i^{(+)}$ and $\tilde{X}_f^{(-)}$ in our distorted wave formulation are in fact the first guess for the Hartree equations of the initial and final channels. For the hydrogen atom-electron system, they ought to be very accurate.

One would expect, that after the first iteration

$$X_{i,f}^{(\pm)} = \tilde{X}_{i,f}^{(\pm)} + \varepsilon X_{i,f}^{(\pm)} \tag{23}$$

and ε, a small number, can be determined via numerical methods. From now on we shall drop the over-bar on the approximate distorted wave-functions. Hence our distorted-wave transition matrix $T_{f \leftarrow i}^{DW}$ can now be expressed as:

$$T_{f \leftarrow i}^{DW} = \left\langle X_f^{(-)} \left| -\frac{1}{r_1} + \frac{1}{|r_2 - r_0|} - U_i(r_1) \right| X_i^{(+)} \right\rangle \tag{24}$$

In the case of exchange scattering, either the prior or post form of the residual interaction may be used, therefore the residual interaction is the same for both the exchange and direct cases.

D. Evaluation of Hartree Potentials

We shall now work out the simplest case for the hydrogenic-Hartree potential, that of the ground state 1S, since it is present throughout the prior residual interaction operator W_i. The other Hartree potential

up to 2p are listed in Table 1.

To evaluate the matrix element

$$\left\langle \psi_{1s}(r_0) \left| \frac{1}{r_{0_1}} - \frac{1}{r_1} \right| \psi_{1s}(r_0) \right\rangle \tag{25}$$

We set r_0 as the polar axis and use the standard expansion in Legendre polynomials

$$\frac{1}{|r_0 - r_1|} = \sum_{n=0}^{\infty} \frac{r_<^n}{r_>^{n+1}} P_n(\cos\theta) \tag{26}$$

where $r_>$ = greater (r_1, r_0); $r_<$ = smaller (r_1, r_0); θ is the angle between r_0 and r_1.

The orthogonality relationship

$$\int_0^{\pi} P_n(\cos\theta)\, P_m(\cos\theta)\, d(\cos\theta) = \frac{2}{2n+1}\, \delta_{nm} \tag{27}$$

gives us the desired result

$$\int d^3 r_0\, \psi_{1s}^*(r_0) \left(\frac{1}{r_{0_1}} - \frac{1}{r_1} \right) \psi_{1s}(r_0) = -e^{-2r_1}\left(1 + \frac{1}{r_1}\right) \tag{28}$$

As we can see the above integral would have more terms in it when higher orders of Legendre polynomials are introduced with orbitals of higher angular momentum. For the Hartree potential of the 2p states it is necessary to select an axis of quantization for the magnetic substates and to use the more general expression

$$\frac{1}{|r_0 - r_1|} = 4\pi \sum_{\ell=0}^{\infty} \sum_{m=-\ell}^{+\ell} \frac{1}{2\ell+1} \frac{r_<^{\ell}}{r_>^{\ell+1}} Y_{\ell m}^*(\theta_0, \tau_0)\, Y_{\ell m}(\theta_1, \tau_1) \tag{29}$$

As expected from electrostatic multipole expansion we obtained an angular dependent Hartree potential. The results are listed below in Table I.

Table 1.

ψ_i	Hartree potential $U_H^i(r_1) = \left\langle \psi_i^*(r_0) \middle\| \frac{1}{r_{0_1}} - \frac{1}{r_1} \middle\| \psi_i(r_0) \right\rangle$
1s	$-e^{-2r_1}(1 + \frac{1}{r_1})$
2s	$-e^{-r_1}\left(\frac{1}{2} r_1^2 + \frac{1}{2}r_1 + \frac{3}{2} + \frac{1}{2r_1}\right)$
$2p_0$	$-e^{-r_1}\left[\left(r_1^2\right)\left(\frac{3}{2} + 2\cos^2\theta_1\right) + r_1\left(\frac{27}{60} + \frac{32}{60}\cos^2\theta_1\right) + \left(\frac{3}{2} + 2\cos^2\theta_1\right) + \left(\frac{6}{r_1} - \frac{2\cos^2\theta_1}{r_1}\right) + \frac{3\cos^2\theta_1}{r_1^2} + \frac{3\cos^2\theta_1}{r_1^3}\right] - \frac{2}{r_1^3} - \frac{\cos^2\theta_1}{r_1^3}$
$2p_{\pm 1}$	$-e^{-r_1}\left[\frac{7}{2}r_1 + \frac{1}{3}r_1 + \frac{4}{3} + \frac{3}{2r_1} + \frac{3}{r_1^2} + \frac{3}{r_1^3}\right]\sin^2\theta_1 \begin{pmatrix}\sin^2\tau_1\\ \cos^2\tau_1\end{pmatrix} - \frac{3}{r_1^3}\sin^2\theta_1 \begin{pmatrix}\sin^2\tau_1\\ \cos^2\tau_1\end{pmatrix}$

Interestingly enough the Hartree potential for the p lobes has a quadrupole-like asymptotic tail[8,18] to it. This is to be expected from the geometrical shape of the p orbital; hence upon multipole expansion there should be higher terms than just the $\ell=0$ component. Also the average position of the 2p electron is farther away than that for 1s or 2s because of its finite angular momentum. Thus physically we would expect the cross section for the 1s→2p process, which corresponds to an optically allowed transition to be greater than for the 1s→2s excitation, which is optically forbidden by parity. This fact and the difference in angular distributions for the two processes have been borne out by various calculations.[8,18]

To improve on the description of the initial asymptotic atomic potential we could have added a polarization potential of the form

$$-\frac{\alpha}{r^4}\left(1 - \exp -\left(\frac{r}{r_0}\right)^n\right) \tag{30}$$

where α is the ground state polarizability for hydrogen atom and is $\frac{9}{2}$ A.U.; r_0 is an arbitrary cut-off distance; n is chosen to be usually 8.

But we feel that the additional effect ought to drastically decrease at small angles and at high energies, where the Eikonal way prevails. Hence we neglected this term.

E. Further Development of the Transition Matrix

The case of direct scattering from 1s→2s is first treated in detail. From Eqs. (17), (18), and (24) we get:

$$T_{f\leftarrow i}^{DW} \alpha \int d^3r_Q \int d^3r_\ell \frac{1}{32\sqrt{2}\,\pi^2} \exp(-r_0) \exp\Big(iK_i\cdot r_\ell - \frac{i}{2K_i}\int_{-\infty}^{z_1} U_H^{2s}(b_1', z_1')dz_1'\Big) \left(\frac{1}{|r_Q - r_\ell|} - \frac{1}{r_1} - U_H^{1s}(r_1)\right)(2-r_0)\exp\left(-\frac{r_0}{2}\right) \exp\left(-iK_f\cdot r_\ell + \frac{i}{2K_f}\int_{z_1}^{\infty} U_H^{2s}(b_1', z_1')dz_1'\right) \tag{31}$$

where U_H^{2s}, U_H^{1s} stand for the respective asymptotic Hartree potentials.

Integrating Eq. (31) over r_Q coordinates and invoking the orthogonality of the bound-state wavefunctions we get only contributions from the $\frac{1}{|r_Q - r_\ell|}$ term which is the following

$$B(r_1) = \left\langle \psi_{2s}(r_0) \left| \frac{1}{|r_0 - r_1|} \right| \psi_{1s}(r_0) \right\rangle$$

$$= \frac{1}{\sqrt{2}} \exp(-\frac{3}{2} r_1)(\frac{16}{9} r_1 + \frac{8}{27}) - \frac{10}{81 r_1}$$

and so $T_{f\leftarrow i}^{DW} \alpha \frac{1}{(2^{11/2})} \frac{i}{\pi^2} \int d^3 r_1 \exp(i K_i \cdot r_1 - \frac{i}{2Ki} \int_{-\infty}^{z_1} U_H^{1s}(b_1', z_1') dz_1' \Big)$

$$B(r_1) \exp(-iK_f \cdot r_1 + \frac{i}{2K_f} \int_{z_1}^{+\infty} U_H^{2s}(b_1', z_1') dz_1'$$

In Table II we list all the $B(r_1)$ for the direct excitation processes $1s \rightarrow 2s, 2p$ considered here.

Table 2.

	$B(r_1) = \left\langle \psi_f(r_0) \left| \frac{1}{\lvert r_0 - r_1 \rvert} \right| \psi_i(r_0) \right\rangle$
$1s \rightarrow 2s$	$\frac{1}{\sqrt{2}} \exp(-\frac{3}{2} r_1)(\frac{16}{9} r_1 + \frac{8}{27}) - \frac{10}{81 r_1}$
$1s \rightarrow 2p_{0,\pm 1}$	$\frac{1}{3\sqrt{2}} \left[\exp(-\frac{3}{2} r_1)(-\frac{2}{3} r_1^2 - \frac{10}{9} r_1 - \frac{24}{9} + \frac{48}{9 r_1} + \frac{91}{3 l r_1^2}) + \frac{96}{3 l r_1^2} \right] \cos\theta_1$

A simple use of the Addition Theorem for spherical Harmonics[17] shows that $B(r_1)$ from rotational symmetry is the same for the three magnetic sublevels of the p level.

The expression in Eq. (31) can further be reduced by integrating in the b and z coordinate systems. So

$$\int d^3 r_1 = \int d^2 b_1 \int dz_1 \qquad (32)$$

and by simplifying the momentum transfer vector relation.

We have for the momentum transfer vector K the relationship:

$$\underset{\sim}{K} = \underset{\sim}{K}_i - \underset{\sim}{K}_f$$

but

$$\underset{\sim}{r} = \underset{\sim}{b}_1 + z_1 \hat{K}_i$$

so let

$$\cos\alpha = \hat{K} \cdot \hat{b}_1$$

where α is the projection of $\underset{\sim}{K}$ on the $\underset{\sim}{b}_1$ vector which lies on the impact parameter plane.

Now

$$K^2 = K_f^2 + K_i^2 + 2K_f K_i \cos\theta$$

where θ is the momentum transfer angle

$$\therefore (\underset{\sim}{K}_i - \underset{\sim}{K}_f) \cdot (\underset{\sim}{b}_1 + z_1 \hat{K}_i) = K b_1 \cos\alpha + z_1(K_i - K_f \cos\theta) \qquad (33)$$

The above equation demonstrates that in the small angle limit the momentum transfer vector is parallel, rather than perpendicular to the final and initial wave-vectors, whereas in the first Born approximation the momentum transfer vector in the small-angle limit is perpendicular to the initial and final vectors. Thus the expression of the transition matrix for direct excitation processes has the extra factor $(K_i - K_f \cos\theta)z_1$ in its exponential argument, unlike the usual Eikonal scattering amplitude expression.

Then the transition matrix element is written as:

$$T_{f\leftarrow i}^{DW} \alpha \frac{1}{2^{11/2}\pi^2} \int_0^{\infty} db_1 b_1 \int_0^{2\pi} d\alpha \int_{-\infty}^{+\infty} dz_1 \exp[i(K_i - K_f \cos\theta)z_1] \qquad (34)$$

$$B(r_1) \exp(iKb_1\cos\alpha) \exp\Big(\frac{i}{2} \Big(\frac{1}{K_f} \int_{z_1}^{+\infty} U_H^{2s} dz_1' - \frac{1}{K_i} \int_{-\infty}^{z_1} U_H^{1s} dz_1' \Big) \Big)$$

Using the fact that

$$J_0(x) = \frac{1}{2\pi} \int_0^{2\pi} e^{-ix\cos\theta} d\theta \tag{35}$$

is the integral representation[17] for Bessel function of the zeroth order, we can further obtain:

$$T_{f\leftarrow i}^{DW} \alpha \frac{1}{(2)^{9/2}\pi} \int_{-\infty}^{+\infty} dz_1 e^{i(K_i - K_f\cos\theta)z_1}$$

$$\int_0^{\infty} db_1\, b_1\, J_0(Kb_1)\, B\left(\sqrt{b_1^2+z_1^2}\right) \tag{36}$$

$$\exp\left[\frac{i}{2}\left(\frac{1}{K_f}\int_{z_1}^{+\infty} U_H^{2s}(z_1',b_1')dz_1' - \frac{1}{K_i}\int_{-\infty}^{z_1} U_H^{1s}(z_1',b_1')dz_1'\right)\right]$$

Next we face the task of evaluating the "Eikonal" phase shifts:

$$\frac{i}{2}\left(\frac{1}{K_f}\int_{z_1}^{+\infty} U_H^{2s}(z_1',b_1')dz_1' - \frac{1}{K_i}\int_{-\infty}^{z_1} U_H^{1s}(z_1',b_1')dz_1'\right) \tag{37}$$

Even for the simplest prior-potential, that of the 1s state, the integral can not be evaluated via analytic means, because conversion to the integral form of Bessel functions is not possible because the upper limit depends on a parameter instead of a finite value. Therefore numerical methods must be used in evaluating the transition matrix, $T_{f\leftarrow i}^{DW}$, for all excitation processes.

To evaluate these integrals numerically, it behooves one to change variable

$$V = \frac{+r_1'}{\sqrt{r_1^2 - b_1^2}}, \tag{38}$$

then the integrals of the Hartree potential $U_H^i(z_1',b_1')$ over the z_1' coordinate for both the incoming and outgoing phase shifts would have

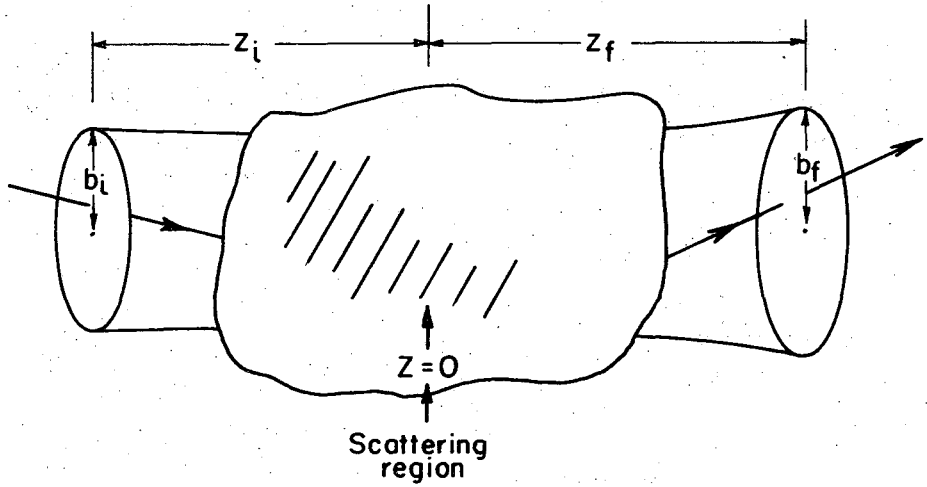

XBL716-6806

Fig. 2. Eikonal trajectory (straight line approximation).

the forms

$$\int_{-\infty}^{+1} e^{-\beta V z_1} f(V,b_1',z_1)dV$$

and (39)

$$\int_{+1}^{+\infty} e^{-\beta V z_1} f(V,b_1',z_1)dV$$

respectively; where β is determined by the appropriate quantum state, and $f(V,b_1',z_1)$ is a simple algebraic expression. Thus for each input values of (b_1', z_1) one would obtain via Simpson's rule[17] the numerical value of the phase-shift.

In the numerical double integration over the b-Z plane, we shall integrate over the area from $-Z^i$ = initial cut-off distance to $+Z^f$ = final cut-off distance, and from $-b^f$ to $+b^f$ and from $-b^i$ to $+b^i$, where the limits of integration are dictated by the strength of the asymptotic Hartree potential. This scheme is shown in Fig. 2. The grid-system to evaluate the double integral ought to be pretty standard. By virtue of the medium-high impact energy, one in short integrates over a "tube"[19] about the classical trajectory, the ends of the "tube" may be different in area, depending on the accuracy of the approximation and the tails of the potential. Indeed, the Eikonal approximation has its origin in optics;[20] in first order it is a straight line approximation much in the spirit of light rays, only in higher order terms does the curvature of the trajectory comes into play.

F. Transition Matrix for Exchange Process

In collision theory exchange processes are usually much harder to formulate and to calculate than direct processes.[13,14] Therefore, it should be no wonder that the transition matrix for exchange in this distorted Eikonal formulation would yield poorer results than for the direct scattering case, but that the result would be superior to the

first Born treatment. This basis for this argument is that straight trajectories are assumed for the first-order Eikonal waves and that the interaction is localised about the scattering site, whereas in the exchange process a non-local exchange potential, usually an integral operator type, is involved. Only the asymptotic wavefunctions $X_i^{(+)}$, $X_f^{(-)}$ are employed, so the Hartree field observed by the exchanged electron would be the same as the direct case, with the exception of having a different coordinate designation. Unlike the direct case, there is no way to reduce the six-dimension integral in the transition matrix element to a three dimensional integral. This is due to the presence of "Eikonal" phase shifts which does not permit one to utilize the integral representation of $\frac{1}{|r_Q-r_1|}$, namely

$$\frac{1}{|r_Q-r_1|} = \frac{1}{2\pi^2}\int d^3K \frac{1}{K^2} e^{i\mathbf{K}\cdot(r_1-r_Q)} \qquad (40)$$

and hence to use the momentum representation of hydrogenic wavefunctions which one could do in the exchange scattering transition matrix for the first Born approximation.[1] Besides the exchange electron's distorted wavefunction is now no longer orthogonal to the initial hydrogenic wavefunction. That is:

$$\int d^3r_Q \exp(i\mathbf{K_f}\cdot r_Q + \frac{i}{2K_f}\int_{z_0}^{\infty} U_H^{2s,2p}(b_0',z_0')dz_0')$$

$$\psi_{1s}(r_0) \neq 0$$

In all two additional terms from the $\frac{1}{r_1}$ and $U_i(r_1)$ interactions are present in the distorted wave transition matrix of the exchange mode.

Formally we can write the exchange contribution in the complete form of:

$$T_{f\leftarrow i}^{DW}\ (\text{exchange}) = \left\langle \psi_{2s,2p}(r_1)\ \exp\ (iK_f\cdot r_Q + \frac{i}{2K_f}\int_{z_0}^{\infty} U_H^{2s,2p}\ (b_0',z_0')\ dz_0') \right.$$

$$\left| -\frac{1}{r_1} + \frac{1}{|r_1 - r_Q|} - U_i(r_1) \right| \psi_{1s}(r_0)$$

$$\left. \exp\ (iK_i\cdot r_Q + \frac{i}{2K_i}\int_{-\infty}^{z_1} U_H^{1s}\ (b_1',z_1')dz_1') \right\rangle \qquad (41)$$

Needless to say, the numerical task for this system in the exchange case is much more difficult than that for direct process, as in all quantum and classical scattering problems.

In extending this approach to electron scattering off slightly larger atoms, say He, Li, Be, one must take into account the correlation effects quantum mechanically among the core and outer shell electrons and the distortion effects on their wavefunctions by the free electron. Certainly tabulated Hartree functions, with correlation taking into account by configuration interactions, would further promote the validity of this distorted Eikonal wave picture for larger atoms, at least in the medium-high energy range.

To conclude this section of the thesis, we can add higher-order correction terms to the first-order distorted Eikonal waves by making additional iterations of the Hartree equations to improve on the potential and by making a second Eikonal approximation[19] which contains in it an amplitude dependent term. In the spirit of the one-dimensional JWKB wavefunction, this new term[21] would serve to measure the curvature of the projectile's path. However, this method may be necessary only at lower energies than the ones considered here.

REFERENCES

1. B. L. Moiseiwitsch and S. J. Smith, Rev. of Mod. Phys. 40, 238 (1968); S. Geltman, Topics in Atomic Collision Theory, Academic Press, New York (1969).
2. W. H. Miller, J. Chem. Phys. 53, 1949 (1970).
3. Bethe and Salpeter, Quantum Mechanics of One- and Two-Electron Atoms, (Springer Verlag, Berlin/Goettingen/Heidelberg, 1957).
4. Truhlar, Cartwright, Kuppermann, Phys. Rev. 175, 113 (1968).
5. E. Corinaldesi and L. Trainor Nuovo Cimento 9, 940 (1952).
6. M. R. H. Rudge, Proc. Phys. Soc. (London) 85, 607 (1965); 86, 763 (1965).
7. D. R. Bates, Proc. Roy. Soc. (London) A247, 294 (1958); R. H. Bassel and E. Gerjuoy, Phys. Rev. 117, 749 (1960); M. H. Mittleman, Phys. Rev. 122, 1930 (1961).
8. P. G. Burke, S. Ormonde and W. Whitaker, Proc. Phys. Soc. (London) 92, 319 (1967); S. Geltman and P. G. Burke, J. Phys. B: Atom. Molec. Phys. 3, 1062 (1970).
9. R. K. Nesbet, Phys. Rev. 179, 60 (1969).
10. G. A. Erskine and H. S. W. Massey, Proc. Roy. Soc. (London) A212, 521 (1952); V. I. Ochkur, Soviet Phys. (JETP) 18, 503 (1964).
11. W. N. Shelton, E. S. Leherissey, and D. H. Madison, Phys. Rev. A 3, 242 (1971); W. N. Shelton et al., J. Phys. B: Atom. Molec. Phys. 4, 71 (1971).
12. A. Messiah, Quantum Mechanics Vol. II (John Wiley & Sons Inc. New York, 1962) pp. 822 ff.
13. L. S. Rodberg and R. M. Thaler, Introduction to the Quantum Theory of Scattering, (Academic Press, New York, 1967).
14. R. G. Newton, Scattering Theory of Waves and Particles (McGraw-Hill

Co., New York, 1966), Chapter 18.

15. L. Pauling and E. B. Wilson, Introduction to Quantum Mechanics (McGraw-Hill Co., New York, 1935).

16. For a good discussion of the Hartree central field method see E. Condon and G. Shortley, The Theory of Atomic Spectra (Cambridge U. P., 1967), pp. 354 ff.

17. J. Matthews and R. L. Walker, Mathematical Methods of Physics (W. A. Benjamin Inc., New York, 1969).

18. M. K. Gailitis and R. Damburg, Proc. Phys. Soc. (London) 82, 192-200, (1963).

19. J. C. Y. Chen and K. M. Watson, Phys. Rev. 174, 152 (1968).

20. H. Goldstein, Classical Mechanics (Addison-Wesley, Reading, Mass., 1950) pp. 311.

21. H. M. Van Horn and E. E. Salpeter, Phys. Rev. 157, 751 (1967).

III. SEMI-CLASSICAL TREATMENT OF ELECTRON-HYDROGEN ATOM SCATTERING

The theme of the final chapter of this thesis is to apply classical dynamics and semi-classical boundary conditions along with appropriate quantum-mechanical superposition of scattering amplitudes in the treatment of low-level excitation of hydrogen atom by impact of electrons. This is especially interesting since for excitation of high quantum numbers,[1] the correspondence principle can be invoked and thus one would expect that quantum and semi-classical (among them the Eikonal approximation[2]) results ought to agree in most details. Our prime goal then lies in quantum number excitations (1s→2s, 2p) around the first threshold region, because it would be neat to see how such a quantum-like system, from the criterion of DeBroglie's wave,[3] would behave under the recently formulated classical $\mathcal{S}$-matrix framework.

A. Other Semiclassical or Classical Treatments of Electron-Atom Scattering

The original classical theories of atomic scattering due to Thomson (1912)[4] and Rutherford (1911)[4] were proposed before quantum mechanics was known. Despite the discovery of quantum mechanics and its wide application to atomic scattering, classical methods continue to be used for their comparative simplicity. The reason for this is that the number of coupled equations that must be solved via classical mechanics correspond to the degrees of freedom of the collision system, while quantum-mechanically one has to solve the appropriate number of coupled Schroedinger equations for the quantum states involved, which even for simple processes very often exceed present day computational capabilities. The close-coupling approximation[5] represents the quantum-mechanical approach to limit the number of atomic states which are in the expansion of the total wavefunction.

Since the development of quantum theory, classical methods were largely neglected until the paper of Gryzinski[6] appeared in 1959. He showed that classical methods could be used to calculate simple and useful analytic approximate cross sections for a variety of processes. Monte-Carlo calculations by Abrines et al. (1966);[1] Brattsev and Ochkur (1967),[7] were also carried out for the ionization of classical hydrogen atoms by electrons. As expected, the result for n=1 does not agree so well as for protons used as projectiles, this is due to the quantum-mechanical interference between direct and exchange electron scattering. Recently Percival and Richards[8] showed how Bohr's correspondence principle could be applied to collision-induced transitions in the weak coupling region where both quantum and classical perturbation theory are valid. They obtained cross sections for transitions between highly excited states of hydrogen atoms induced by electron impact.

The above classical methods have an inherent ambiguity in the choice of boundary conditions, because in representing quantum mechanical states by classical distributions, one encounters the uncertainty principle in position and momentum. However, as we shall see below, the recently developed classical $\int$-matrix theory shows how the appropriate use of classical mechanical canonical transformations, the cousins of quantum mechanical unitary transformations, would yield the proper initial conditions for the classical equations of motion for each degree of freedom of the system.

B. Capsule Presentation of the Classical $\int$-Matrix Formalism

Here we shall give the basic development and motivation of the classical $\int$-matrix formalism developed by W. H. Miller.[9] The finer details of much of what follows in this section can be found in Miller's[16] investigations of the role played by classical and quantum mechanics in

molecular collision dynamics.

R. P. Feynman[3] in his far-out development of quantum mechanics by means of path integrals, whose origin can be traced to Wiener,[11] linked classical mechanics with quantum mechanics by showing that the quantum-mechanical propagator for spatial representation in the classical limit is

$$\langle q_2|e^{-iH(t_2-t_1)/\hbar}|q_1\rangle \sim \sum_{\substack{\text{all classical}\\ \text{paths}}} e^{i[i\phi(q_2,q_1)]/\hbar} \qquad (1)$$

where $q_2 \equiv q(t_2)$, $q_1 \equiv q(t_1)$ are the values of the coordinate at times t_2, t_1, H is the time independent Hamiltonian governing the system and ϕ is the classical action integral between two space-time points

$$\phi(q_2,q_1) = \int_{t_1}^{t_2} dt\, L[q(t),\dot{q}(t)] \qquad (2)$$

L is the classical Lagrangian of the system and $q(t)$, $\dot{q}(t)$ obey the classical equations of motion.

It is important to note that since q_1, q_2 are the independent variables which specify the classical trajectory, the trajectory may not be unique, hence there may be several classical paths with q_1 fixed which lead to the same value of q_2, whereas if q_1 the coordinate and p_1 the canonical momentum are specified at time t_1, then $q(t)$, $p(t)$ are uniquely determined for all later times. This fact arises from the variational derivation of Hamilton's equations.

It is interesting to point out that where q are the spatial coordinates of one set of canonical variables and P are the constants of motion of another set, then $F_2(q,P)$,[13] a generator of classical canonical transformation, is the solution to the familiar Hamilton-Jacobi equation.[12,13] More concisely in quantum-mechanical language, this action principle concept may be expressed as:

$$\psi_E(x) = \langle x|E\rangle = \langle q|P\rangle \sim e^{iF_2(q,P)}$$

$$\text{so } \psi_E(x) \sim \psi_{WKB}(x) \tag{3}$$

It is also easy to show that if the Hamiltonian does not involve time explicitly, then

$$\frac{\partial^2 F_2}{\partial q \partial P} \sim \frac{1}{\sqrt{K(X)}} \tag{4}$$

for the correct WKB amplitude dependence.[14]

Now the classical $\int$-matrix can be found from evaluating the matrix elements of the operator $\int$ from some initial eigenstate of H_0 to a final eigenstate of H_0; H_0 is the Hamiltonian for the collision partners at asymptotic distances. From formal quantum scattering theory[3]

$$\int = \lim_{\substack{t_2\to+\infty \\ t_1\to-\infty}} e^{iH_0 t_2/\hbar}\, e^{-iH(t_2-t_1)/\hbar}\, e^{-iH_0 t/\hbar} \tag{5}$$

where H is the total Hamiltonian governing the collision system. From semi-classical reasoning, one sees that from the old quantum theory[15] the momenta or action variables, being constants of the motion of H_0, are the precise classical equivalent of quantum numbers in quantum mechanics and the conjugate angle variables are the quantum phase angles. In scattering problems one prefers the $\int$-matrix in the momentum representation of these variables.

Since $|p\rangle$ are eigenstates of H_0 then

$$e^{\pm i H_0 t/\hbar}\,|p\rangle = e^{\pm iEt/\hbar}|p\rangle \tag{6}$$

Then the $\int$-matrix is related to the propagator or evolution operator in the momentum representation by

$$\lim_{\substack{t_2\to+\infty \\ t_1\to-\infty}} \langle p_2|\int|p_1\rangle = \lim_{\substack{t_2\to+\infty \\ t_1\to-\infty}} e^{iE(t_2-t_1)/\hbar}\, \langle p_2|e^{-iH(t_2-t_1/\hbar}|p_1\rangle \tag{7}$$

Using the fact that the Hamiltonian is related to the Lagrangian by $H(p,q) = pq - L(q,\dot{q})$ and writing the phase of the propagator, $\phi(q_2,q_1)$, in the momentum representation, $\phi(p_2,p_1)$, we have finally in terms of the phase of the classical propagator in the momentum representation: The classical $\int$-matrix[10] is given by

$$\langle p_2|\int|p_1\rangle = \sum_{\substack{\text{all classical} \\ \text{paths}}} \left[2\pi\left(\frac{\partial p_2}{\partial q_1}\right)_{p_1}\right]^{-1/2} e^{i\phi(p_2,p_1)} \tag{8}$$

The appropriate classical-limit normalization $\left[2\pi\left(\frac{\partial p_2}{\partial q_1}\right)_{p_1}\right]^{-1/2}$ has been physically interpreted in terms of its square modulus $(2\pi)^{-1}\left|\frac{\partial q_1}{\partial p_2}\right|_{p_1}$. This is verily the probability of the $p_1 \to p_2$ transition associated with a particular trajectory.

$\phi(p_2,p_1)$ is obtained from $\phi(q_2,q_1)$ by simple rules of unitary transformation and is found to be:

$$\phi(p_2,p_1) = -\int_{t_1}^{t_2} dt\; q(t)\,\dot{p}(t) \tag{9}$$

where q(t), p(t) obey Hamilton's equations i.e.

$$\frac{dq(t)}{dt} = +\frac{\partial H(p,q)}{\partial p} \quad \text{and} \quad \frac{-dp(t)}{dt} = \frac{\partial H(p,q)}{\partial q} \tag{10}$$

The above developed expression for the classical $\int$-matrix is for one degree of freedom and one pair of canonical coordinate and momentum, it can be extended to any number of degrees of freedom without too much effort.

In continuing this semi-classical spirit, to obtain the transition

$P_{1,2}$ from state 1 to state 2, we calculate the dynamics of the interacting system via classical mechanics and treat the transition amplitude according to well-posed quantum superposition postulates.

To arrive at $P_{1,2}$ quantum mechanically one calculates the $\int_{1,2}$, $\int$-matrix element, via quantum dynamics, i.e. Schroedinger equation, and square the $\int$-matrix element to obtain the transition probability $P_{1,2}$

$$P_{1,2} = |\int_{1,2}|^2 \tag{11}$$

From the classical $\int$-matrix expression in Eq.(11) we see readily that the transition probability in this semi-classical approach $P^{SC}_{1,2}$ can be decomposed principally into two parts, one having a particle-like or classical origin, the other having a wave-like or quantum-mechanical nature. Namely

$$P^{SC}_{1,2} = P^{CL}_{1,2} + P^{QM}_{1,2}$$

$$P^{CL}_{1,2} = \sum_{\substack{\text{all classical} \\ \text{paths}}} p_i \tag{12}$$

where the p_i's are probabilities (obtained by solving classical equations of motion) associated with all the possible classical trajectories, and $P^{QM}_{1,2}$ are the cross-interference terms when one squares the classical $\int$-matrix element.

$$P^{QM}_{1,2} = 2 \sum_i \sqrt{p_i}\, e^{-i\phi_i} \sum_{i \neq j} \sqrt{p_j}\, e^{i\phi_j} \tag{13}$$

where the sum, once again, is taken over all classical trajectories. The terms $e^{i(\phi_j - \phi_i)}$ give the transition probability $P^{SC}_{1,2}$ the wave-like behavior which pure classical approaches miss. This is the <u>quantum effect</u> of the classical $\int$-matrix outlook.

Furthermore from conservation of probability $P^{SC}_{1,2}$ can be divided into the direct (non-reactive, NR) part and the exchange (reactive, R) part.

$$\therefore P^{SC}_{1,2} = \sum_{p_2} P^{NR}_{p_2,p_1} + \sum_{p_2} P^{R}_{p_2,p_1} \tag{14}$$

The result from sweeping the q_1 from 0 to 2π, as it has been noted before, is exactly the same as a <u>Monte-Carlo</u>[16] averaging over a large number of appropriately chosen classical trajectories.

C. <u>The Classical Hamiltonian for the Electron-Hydrogen Atom System</u>

Now we shall apply the above-delineated method to the three problem of the electron-hydrogen atom system, alias the "helium" atom kid.

The electron-hydrogen atom system classically has nine degrees of freedom. Transforming to the center of mass (CM) system by means of a contact transformation and using the fact that the integrals of motion of the center of mass are constants, the transformed system then has six degrees of freedom. (See Appendix I.) Further reduction to four degrees of freedom is made by virtue of the conservation of total angular momentum and its component along some fixed-space axis analogons to the commutation relations $[H,Jz] = 0$, $[H,J^2] = 0$, where H is the total quantum-mechanical Hamiltonian. This is accomplished via a $F_3(Q,p)$ transformation and the use of the constants of motion of the total angular momentum. Thus the three body problem is at last reduced to four degrees of freedom.[17]

For physical reasons that now the new Hamiltonian system represents the equations of motion of two particles, one being the target or the hydrogen atom, the other the projectile or the free electron, we choose the four pair of canonical variables as the following:

$$p_1 = p_2 \qquad q_1 = R$$
$$p_2 = p_r \qquad q_2 = r$$
$$p_3 = j \qquad q_3 = q_j \qquad (15)$$
$$p_4 = \ell \qquad q_4 = q_\ell$$

where R is the radial coordinate between the electron to the center of mass of the hydrogen atom; r is the radial coordinate between the bound electron and proton; p_r, p_R are translational radial momenta corresponding to their conjugate coordinates; ℓ is the orbital angular momentum of the projectile electron with respect to the atom; j is the rotational angular momentum of the bound electron about the proton; q_j,q_e are the angles, between 0 and 2π, conjugate to these angular momenta.

In terms of these canonical variables the classical Hamiltonian is given as[17]

$$H(p,q) = \frac{1}{2\mu}\left(p_R^2 + \frac{\ell^2}{R^2}\right) + \frac{1}{2m}\left(p_r^2 + \frac{j^2}{r^2}\right) + v(r) + V(r,R,\gamma) \qquad (16)$$

where μ is the reduced mass of the projectile

$$\mu = \frac{m_e(m_p+m_e)}{m_p+2m_e} \approx m_e$$

m is the reduced mass of the target

$$m = \frac{m_p m_e}{m_p+m_e} \simeq m_e$$

$v(r) = -\frac{e^2}{r}$, the exact electro-static potential of the hydrogen atomic system.

$V(r,R,\gamma)$ is the electrostatic interaction potential between the free electron and hydrogen atom; γ is the angle between $\underset{\sim}{r}$ and $\underset{\sim}{R}$ in which the interaction potential $V(r,R,\gamma)$ is expressed.

In terms of the canonical variables

$$\cos\gamma = \cos q_j \cos q_\ell + \frac{[\ell^2+j^2-J^2]}{2\ell j} \sin q_j \sin q_\ell \qquad (17)$$

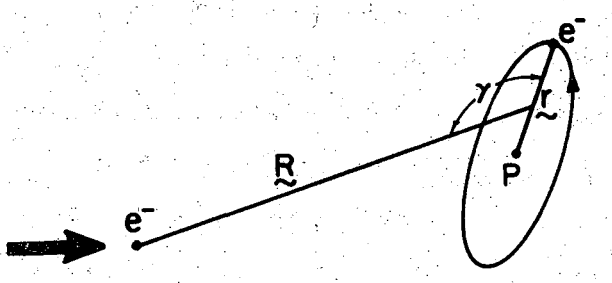

XBL716-6805

Fig. 1. Electron-hydrogen atom reduced to four degrees of freedom.

where J is the total angular momentum of the system and J = ℓ+j, and a constant of the motion.

For our simple atomic problem we can in fact write out V(r,R,γ) in closed form as:

$$V(r,R,\gamma) = -e^2(r^2+R^2-2rR\cos\gamma)^{-1/2} + e^2(r^2+R^2+2rR\cos\gamma)^{-1/2} \quad (18)$$

The physical situation of the problem is shown in Fig. 1.

The asymptotic limit of this interaction potential V(r,R,γ) is different for the classical electrostatic case and the quantum electronic distribution obtained from Schroedinger perturbation theory. This important point will be discussed in the later section pertaining to trajectory calculations.

Moving in the semi-classical trend, we shall quantize by means of the Bohr-Sommerfeld quantum conditions the rotational and vibrational degrees of freedom for the hydrogen atom (our "diatom") system.

We have from the old quantum mechanics[14]

$$(n+\tfrac{1}{2})\pi = \oint p_i \, dq_i \quad (19)$$

where n is an integer 0,1,2,... and i is an index for each degree of freedom. So for the relative translational momentum between the bound electron and proton we can state

$$(n+\tfrac{1}{2})\pi = \int_{r<}^{r>} dr \sqrt{2m[\varepsilon(n,j)-V(r)] - \frac{j^2}{r^2}} \quad (20)$$

where r< , r> are the classical turning points of the vibration motion of the bound electron about the proton. Physically, the vibration degree of freedom classically corresponds to the radial quantum number n_r in quantum mechanics, while the rotational degree of freedom can be likened to the quantum number ℓ. The generator $F_2(q,P)$ which gives the desired

quantized conditions can be seen to be:[10]

$$F_2(q,P) = Rp_R + q_j j + q_\ell \ell \pm \int_{r<}^{r} dr' \sqrt{2m[\varepsilon(n,j) - V(r')] - \frac{j^2}{r'^2}} \quad (21)$$

where the first three terms are just the identity transformation, and the last term arises from the particular quantized condition and is readily seen to be related to the WKB wavefunction of the hydrogen atom.[23]

For the Coulomb potential $V(r) = \frac{-e^2}{r}$ it is not difficult to show from the implicit eigenvalue relation in Eq. (20) that in terms of atomic units

$$\varepsilon(n,j) = -\frac{1}{2(n+j+1)^2} \quad (22)$$

From the usual WKB reasons the conditions for n,j are $n = -\frac{1}{2},0,\frac{1}{2},\ldots$ and $j = -\frac{1}{2},0,\frac{1}{2},\ldots$

It is also not surprising to see that the physical systems whose eigenvalues can be solved exactly by Schroedinger equation, these same eigenvalues can be solved via semi-classical (WKB) eigenvalue relationships. So for the case of the one-dimensional harmonic oscillator one obtains with Eq. (19) the correct quantum-mechanical energy relationship $(n+\frac{1}{2})\hbar\omega$; for the case of the one-dimensional Morse potential, $D[e^{-2a(r-r_0)} - 2e^{-a(r-r_0)}]$ one performs the WKB phase integral and obtains the eigenvalue

$$\varepsilon(n) = -D\left(1 - \frac{2n+1}{2\left(\frac{2mD}{\hbar^2 a^2}\right)^{1/2}}\right)^2 \quad (23)$$

the same as for the quantum case.[18]

Using the generator $F_2(q,P)$ as shown above in Eq. (21), we find that for the quantized condition imposed the new canonically transformed

Hamiltonian is

$$H = \frac{1}{2\mu}\left(p_R^2 + \frac{\ell^2}{R^2}\right) + \varepsilon(n,j) + V(r,R,\gamma) \tag{24}$$

From the definition

$$\frac{\partial F_2}{\partial P_i}(q_i,P_i) = Q_i$$ [13]

we see that:

$$q_n = m\,\frac{\partial \varepsilon(n,j)}{\partial n}\int_{r<}^{r} dr' \frac{1}{\left(2m[\varepsilon(n,j)-V(r')] - \frac{j^2}{r'^2}\right)^{1/2}} \tag{25}$$

and

$$\tilde{q}_j = q_j - (-1)^{\left[\frac{q_n}{\pi}\right]}\int_{r<}^{r(n,j,n)} \frac{dr'\left[m\,\frac{\partial \varepsilon(n,j)}{\partial j} - \frac{j}{r'^2}\right]}{\left(2m[\varepsilon(n,j)-V(r')] - \frac{j^2}{r'^2}\right)^{1/2}} \tag{26}$$

where $\left[\frac{q_n}{\pi}\right]$ is the greatest integer function.

To rid of the ungainly "phase shift" in $\tilde{q}_j$, we use the fact that

$$\frac{\partial(n+\frac{1}{2})}{\partial j} = 0$$

which implies then

$$\frac{\partial}{\partial j}\int_{r<}^{r>} dr \sqrt{2m\,\varepsilon(n,j)-V(r') - \frac{j^2}{r'^2}} = 0 \tag{27}$$

So we choose q_n such that $r(n,j,q_n) = r>$ then the "phase shift" vanishes and

$$\tilde{q}_j = q_j \tag{28}$$

The generalized coordinates q_n, q_j, q_ℓ are the angle variables and have value between 0 and 2π, and the corresponding conjugate momenta

n,j,ℓ are the indices for the classical $\mathcal{J}$-matrix. From the total parity of the Hamiltonian the substitution $q_\ell \to q_\ell + \pi$ and $q_j \to q_j + \pi$ leaves the classical Hamiltonian invariant; so we can further restrict[10] the values of q_ℓ from $0 \leq q_\ell \leq \pi$, while q_j remains at $0 \leq q_j \leq 2\pi$.

D. Initial Conditions for Hamilton's Equations

Since the total angular momentum J, $J = \ell + j$, and the total energy E are constants in the collision dynamics, we shall denote our initial $\mathcal{J}$-matrix indices by ℓ_1, j_1, n_1 and vary the corresponding angle variables $q_{\ell_1}, q_{j_1}, q_{n_1}$ over the appropriate intervals. R_1 is required to be large and by energy conservation it is:

$$P_1 = -\left(2\mu[E-\varepsilon(n,j)-V(r_1,R_1,\gamma_1] - \frac{\ell_1^2}{R_1^2}\right)^{1/2} \tag{29}$$

Similarly for the isolated "diatom" (hydrogen atom)

$$P_1 = \pm\left(2m[\varepsilon(n_1,j_1) - \frac{1}{r_1} - \frac{j_1^2}{r_1^2}\right)^{1/2} \tag{30}$$

where r_1 is chosen to be either the perihelion or the apehelion of the Bohr orbit,[15] in order that $\tilde{q}_j = q_j$, for the reason mentioned above.

In order to insure that r_1 is at a turning point, it is necessary to vary R_1, so we shall introduce a phase-shift in the vibration period by moving the projectile either forward or backward for this purpose. We have

$$R_1 = R_0 + \frac{P_1}{\mu\left(\frac{\partial \varepsilon(n,j)}{\partial n}\right)_{n_1}} q_{n_1} \tag{31}$$

$$R_1 = R_0 - \frac{2P_1(n_1+j_1+1)^3}{\mu}\, q_{n_1} \tag{32}$$

where R_0 is to be determined from the nature of the asymptotic interaction potential $V(r,R,\gamma)$ to be discussed in detail in the next section. So we can now vary the phase angles q_j for the numerical computation. In fact q_ℓ, q_j, q_n contain in themselves information about the geometrical orientation of the three bodies with respect to each other.[15]

However, in the Hamilton equations $\dot{q}_\ell = \frac{\partial H}{\partial \ell}$ and $\dot{q}_j = \frac{\partial H}{\partial_j}$ there is a singularity[10] in q_j and q_ℓ as j or ℓ becomes vanishingly small. So instead of integrating Hamilton's equations in the transformed canonical variables (P,Q), it is more prudent to integrate them in Cartesian coordinates (p,q). Thus the initial conditions are specified in terms of action-angle variables as specified above, but then these are transformed to ordinary Cartesian coordinates and the numerical integration of the classical trajectories is carried out by the Adams Moulton technique.[19] At the end of each trajectory one transforms back to the action-angle variables, so with energy and angular-momentum conservation, the trajectory functions $n_2(q_{\ell_1}, q_{j_1}, q_{n_1})$, $j_2(q_{\ell_1}, q_{j_1}, q_{n_1})$, $\ell_2(q_{\ell_1}, q_{j_1}, q_{n_1})$ are obtained and can be used to construct the proper classical $\int$-matrix element. In Appendix I one can find the transformation between the action-angle variables and Cartesian coordinates.

E. Asymptotic Interaction Potential Between an Electron and a Bohr-Quantized Hydrogen Atom

Since classical mechanics is used to describe the dynamics of the collision system, while the boundary conditions are handled with semi-classical methods, it becomes necessary to look at the electrodynamics of the three charged particles subjected to the Bohr-Sommerfeld quantization rules.[14,15] From previous quantum mechanical calculations[20] of the electron-hydrogen atom scattering it has been found that an asymptotic tail from the Coulomb potential is present and it necessitated the

numerical integration of Schroedinger's equation to many a A.U., (sometimes 30 to 50). In order to facilitate computation, it behooves one to investigate the asymptotic nature of the interaction potential $V(r,R,\gamma)$, subjected to classical electrodynamics. For the 1s ground state, there is a big difference in the asymptotic potential between the purely quantum mechanical picture and the classical picture. For higher quantum states the classical treatment and the quantum treatment yield the same form for the potential at far-off distances. The crux of the whole matter lies in the presence of a permanent dipole of the hydrogen for all states when classical mechanics is applied. It is well known that from rudimentary quantum calculations[21] that there is no permanent dipole for the 1s state in a Stark field because of degeneracy, all higher quantum states have a permanent dipole in the presence of an external electric field (for the n=2 $\frac{\psi_{2s} \pm \psi_{2pz}}{\sqrt{2}}$, for n=3 $\frac{\left(\psi_{3s} + \psi_{3d_z{}^2} - \psi_{3p_z}\right)}{\sqrt{3}}$, etc., the z axis being the direction of the external field. Physically, for asymptotic distances, the free electron produces a perturbing potential of the form $H' = eEz$ where E, the electric field, is equal to $\frac{e}{R^2}$, R a certain prescribed asymptotic distance. This perturbing field can be described as a Stark field, since the divergence of the electric field of the free electron in the neighborhood of the hydrogen atom is small. This distorts the hydrogen atom's charge density such that $V_{asymp}(r,R,\gamma) \sim \frac{p}{R^2}$ where p is the dipole moment for that perticular Bohr quantum state. It is well known that, in the quantum mechanical adiabatic approximation,[22] the potential $V(r,R,\gamma)$ seen at large distances from a hydrogen atom is $-\frac{\alpha}{2r^4}$, where α is the polarizability for the quantum state and is related to the induced dipole moment by $\underset{\sim}{p} = \underset{\sim}{\alpha} \cdot \underset{\sim}{E}$, $\underset{\sim}{E}$ the applied electric field, $\underset{\sim}{\alpha}$ the tensor of polarizability.

A closer look at the Bohr picture for the hydrogen atom for the 1s state shows that there exists a permanent dipole. Introducing the polar coordinate notations for a Keplerian orbit subjected to an attractive $\frac{1}{r}$ potential, we can find the average position of the Bohr-quantized electron by integrating over one period of motion.

We have

$$\langle \underset{\sim}{f} \rangle = \frac{\int_0^{2\pi} \underset{\sim}{f}\, r^2\, d\phi}{\int_0^{2\pi} \underset{\sim}{f}\, d\phi} \tag{33}$$

where f is the orbit of the bound electron under no perturbed field.

It can be shown from celestial mechanics[15] that

$$\langle \underset{\sim}{f} \rangle = \frac{3}{2}\, \varepsilon a \hat{\xi} \tag{34}$$

where $\hat{\xi}$ is the perihelion unit vector, ε is the eccentricity of the ellipse and a the semi-major axis of the ellipse. Hence, with the proton being one of the focus, the permanent dipole moment present in a classical Bohr hydrogen atom is $\underset{\sim}{p} = \frac{3}{2}\, \varepsilon a \hat{\xi}$. The secular motions of the hydrogen atom in a Stark field have been investigated in the 1920's by Born and co-workers.[15] Then the use of <u>first-order</u> classical perturbation theory is applied to the Hamilton-Jacobi equations, the result of the perturbed dipole moment is

$$|p| = e\bar{z} = + e \sin q_j \, \frac{3}{2}\, \varepsilon a \sqrt{1 - \left(\frac{jz}{j}\right)^2} \tag{35}$$

where q_j is the angle between the line from the focus to the perihelion and the node of the new plane of orbit subjected to the Stark field and the invariable plane, (r,θ) plane. Historically, the application of the old quantum mechanics to the Stark effect on the spectra of the hydrogen atom yielded the same result as that calculated by Schroedinger[23]

in his first few papers on wave-mechanics.

Next we shall look at the relative magnitude between the first two terms, the dipole and quadrupole terms, of the multiple expansion of $V(r,R,\gamma)$. It is instructive to compare the values p and α in a Taylor series expansion of the energy in an applied electric field $\underset{\sim}{E}$.

$$W(E) = W(0) + \underset{\sim}{p}\cdot\underset{\sim}{E} + \frac{1}{2}\, \alpha E^2 + O(E^3) \tag{36}$$

The values for p,α as a function of parabolic quantum numbers can be calculated from Schroedinger perturbation theory; they are listed in Bethe and Salpeter;[23] from this we get:

$$\frac{\frac{\alpha}{2} E^2}{pE} = \frac{\alpha/2R^4}{p/R^2} = n^4 \frac{\left[17n^2 - 3(n_1-n_2)^2 - 9m^2 + 19\right]}{24n(n_1-n_2)R^2} \tag{37}$$

where $n = n_1+n_2+m+1$ are the quantum numbers one obtains from solving the hydrogen atom problem with parabolic coordinates.

For the case $n=2$, $n_1=1$, $m=0$ which in the spherical-polar coordinate representation corresponds to

$$\langle \underset{\sim}{r} | \psi \rangle = - \frac{1}{\sqrt{2}} \left[R_{20}(r)\, Y_{00}(\Omega) + R_{21}(r)\, Y_{10}(\Omega) \right] \tag{38}$$

The above ratio becomes one when $R \sim 1.5\times10^{-8}$ cm which clearly is not in the asymptotic region. So we shall be concerned only with the dipole attractive term in the far-distant region. Furthermore one can generalize that within an order of magnitude

$$\left.\frac{V(\text{quadrupole})}{V(\text{dipole})}\right|_{QM} \sim \left.\frac{V(\text{quadrupole})}{V(\text{dipole})}\right|_{\text{Classical Bohr orbit}} \tag{39}$$

For the same quantum numbers $n(n_r)$, $\ell(j)$ where n, ℓ are the quantum

labels and n_r and j are old semi-classical indices.[24]

Next we shall give a numerical estimate for the Bohr 1s state. From the semi-classical approximation[14] the $(j+\frac{1}{2})^2$ in the centrifugal potential keeps the electron in the S state where j=0 from falling into the nucleus. It can be derived from application of the old quantum theory[24] that for the hydrogenic system the eccentricity of the orbit $\varepsilon = \sqrt{1 - \frac{j^2}{n^2}}$ and the semi-major axis $a = n^2 a_0$, where n the <u>principal quantum number</u> $n = n_r + j$ and a_0 is the common Bohr radius $a_0 = 0.529$ Å. A semi-classical approximation is then applied to the parabolic quantum numbers, much in the same mode of the spherical quantum numbers.

From the Coulomb degeneracy

$$\begin{aligned} n &= n_1+n_2+1+m \qquad \text{for parabolic system} \\ n &= n_r+j+1 \qquad \text{for spherical system} \end{aligned} \tag{40}$$

n_1 and n_2 are separation constants from Schroedinger equation. When $n_1 \neq n_2$, then there is an asymmetric distribution of charge about the plane z=0, which is the desired effect for a Stark field.

Now for 1s state, $j=\frac{1}{2}$, $n_1 \neq n_2$ and n=1 which implies $m = \pm |\frac{1}{2}|$, $n_1 = \begin{pmatrix} \pm |\frac{1}{2}| \\ 0 \end{pmatrix}$, $n_2 = \begin{pmatrix} 0 \\ \pm |\frac{1}{2}| \end{pmatrix}$. From quantum calculations $p = \frac{3}{2} n(n_1-n_2)$, so a reasonable approximation for the dipole moment for the classical 1s state is $\frac{3}{4}$ A.U. or about 0.39 Debye for our "diatomic" molecule. From the symmetry of the "diatomic" orientation of a rigid rotor, there is no contribution to $V(r,R,\gamma)$ from odd multipoles; i.e. $V(r,R,\gamma) = V(r,R,\pi-\gamma)$. Thus in the classical trajectory calculations, varying the angle q_j at the start would have the effect of orienting the initial static dipole from 0 to π for the incoming electron to scatter from.

After establishing the fact that the asymptotic attractive potential is predominantly of a dipole nature, aside from the always present centrifugal tail, we can solve for the trajectory of the electron

(incident or emergent) subjected to both the repulsive centrifugal and the attractive dipole potentials in the asymptotic region with the orbit equation.[13] We get

$$\theta = \int_0^u \frac{du'}{\sqrt{\frac{2mE}{\ell^2} + \left(\frac{2me\ p}{\ell^2} - 1\right) u'^2}} \tag{41}$$

where $u' = \frac{1}{r'}$, p is the static asymptotic dipole moment to first order

$$p = \frac{3}{2} \varepsilon\ a \sin q_j \sqrt{\left(1 - \frac{j_z}{j}\right)^2} \tag{42}$$

In atomic units where $e = m = \hbar = 1$ then it can be integrated to give:

For the case where

1. $\frac{2p}{\ell^2} - 1 < 0$

$$\theta = \frac{-1}{\sqrt{1 - \frac{2p}{\ell^2}}} \sin^{-1}\left(\frac{\left(\frac{2p}{\ell^2} - 1\right)\frac{1}{r}}{\sqrt{\frac{2E}{\ell^2}\left(1 - \frac{2p}{\ell^2}\right)}}\right) \tag{43}$$

2. $\frac{2p}{\ell^2} - 1 > 0$

$$\theta = \frac{1}{\sqrt{\frac{2p}{\ell^2} - 1}} \sinh^{-1}\left(\frac{\left(\frac{2p}{\ell^2} - 1\right)\frac{1}{r}}{\sqrt{\frac{2E}{\ell^2}\left(\frac{2p}{\ell^2} - 1\right)}}\right) \tag{44}$$

3. $\frac{2p}{\ell^2} - 1 = 0$, using L'Hospital's rule

$$\theta = \sqrt{\frac{\ell^2}{2E}}\ \frac{1}{r}$$

For the input values $p = \frac{3}{4}$ A.U., the Bohr 1s dipole moment; $E = \frac{3}{4}$ A.U., the first threshold energy; and $\ell=1$, the deflection angle obtained from infinity to 10 A.U. is around 10°. Clearly this "spurious" deflection angle would mean the following:

1. The cut-off distances for the numerical integration must be

increased.

2. Both an increase in the total energy E and in the orbital angular momentum ℓ would minimize this undesirable effect from the ls dipole tail.

In Appendix II a way of numerically obtaining the deflection angle in this classical scheme is shown for the case when one employs the body-fixed axes, so as to eliminate many a cross term in the $\underset{\sim}{j}$ and $\underset{\sim}{\ell}$ of the classical dynamics. Also in the appendix a flow chart for the calculation, using both the appropriate analytic expression obtained from the orbit equation and the numerical calculation for the scattering region is given.

In the actual calculation one would then start off with minimum asymptotic distances R_1 and R_2 as shown in Fig. 2 and move them farther away, keeping all other variables constant, until the final n,j,ℓ stabilize. So one would need only to integrate numerically from $R=R_1$ to $R=R_2$, and the tail-end can be followed by the analytic forms. This is very much in the spirit of the Jeffreys-Born approximation.[25] In this adiabatic picture, we assume that essentially we have a static dipole potential, whose time-average over a period of revolution yields the proper orientation q_j, and inclination $\sqrt{1-\left(\frac{j_z}{j}\right)^2}$, etc. Hence the bound electron makes many revolutions, as the projectile traverses in the asymptotic region.

F. Phase of the Classical $\int$-matrix and Quantum Consequences

In an earlier section we see how the phase of the $\int$-matrix was derived. The physical interpretation one can lend to the computed value of the phase may be stated as the number of periods all the degrees of freedom undergo in the collision process. For systems subjected to complex formation or resonance one would expect the value

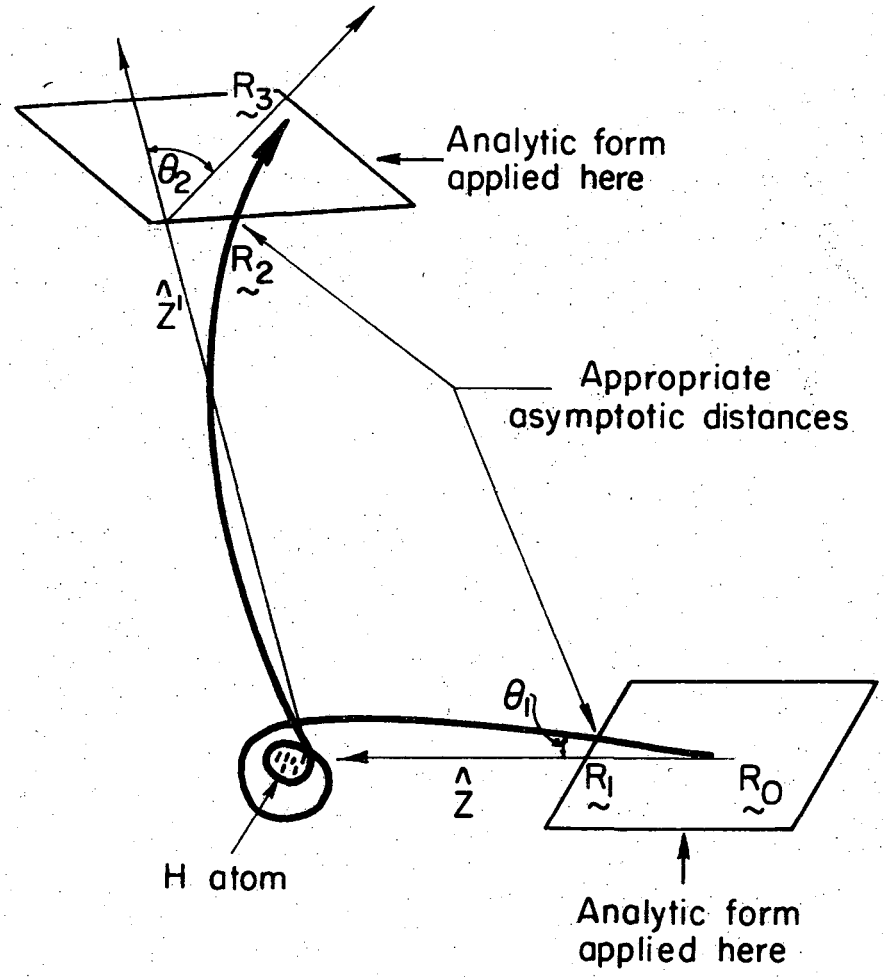

XBL 716-6804

Fig. 2. Sketch of possible trajectory.

to be large in comparison to the value computed for a simple collision process. This is evident in the recent calculations of Rankin and Miller[26] on the $H + Cl_2 \rightarrow HCl + H$ reaction where complex formation is noted, and in Miller's[10] work on the one dimensional $He + H_2$ inelastic collision, where the process is rather simple. Hence the many states of resonance in hydrogen atom would reveal themselves in the case of classical-orbiting[2] or quantum tunneling. In Appendix III the phase of the $\int$-matrix for both the direct and exchange processes in the momentum representation is given for the electron-Bohr hydrogen atom scattering problem where both an analytic form and numerical integration are used to compute the trajectories. For the three dimensional case the classical $\int$-matrix for both exchange and direct processes can be generalized as

$$\int^{(J)}_{n_2,j_2,\ell_2;n_1,j_1,\ell_1} = \sum_{\substack{\text{all classical} \\ \text{paths}}} D^{-\frac{1}{2}} \exp\left(i\phi_{n_2,j_2,\ell_2;n_1,j_1,\ell_1}\right) \qquad (45)$$

where the normalization D, according to prescribed formulation for n degrees of freedom,[10] is given by the Jacobian of the final momenta with respect to the initial coordinates (at fixed initial momenta):

$$D^{-1} = \begin{vmatrix} \frac{\partial n(t_2)}{\partial q_n(t_1)} & \frac{\partial n(t_2)}{\partial q_j(t_1)} & \frac{\partial n(t_2)}{\partial q_\ell(t_1)} \\ \frac{\partial j(t_2)}{\partial q_n(t_1)} & \frac{\partial j(t_2)}{\partial q_j(t_1)} & \frac{\partial j(t_2)}{\partial q_\ell(t_1)} \\ \frac{\partial \ell(t_2)}{\partial q_n(t_1)} & \frac{\partial \ell(t_2)}{\partial q_j(t_1)} & \frac{\partial \ell(t_2)}{\partial q_\ell(t_1)} \end{vmatrix} \qquad (46)$$

where the elements of the Jacobian matrix are simply the numerical value of the slopes of the final momenta with respect to the initial

coordinates. Since electron are Fermions, the quantum-statistical rule[3] on summing of transition amplitudes, in our case classical obtained, yield the relation for the transition probability:

$$P_{f\leftarrow i} = \left| \sum_{\substack{\text{all direct} \\ \text{paths}}} \int_{f\leftarrow i} - \sum_{\substack{\text{all exchange} \\ \text{paths}}} \int_{f\leftarrow i} \right|^2 \qquad (47)$$

In this way, one hopes that the interference between the two kinds of paths would reveal some quantum details.

In conclusion, because of the very quantum-like nature of the electron-hydrogen atom system one might expect possible breakdown of this semi-classical theory. From the DeBroglie's wavelength of the incident electron, for energy of $\frac{3}{4}$ A.U., $\lambda\!\!\!^{-} \sim 1.1$ A.U., we consider the question in terms of simple one-dimensional barrier arguments and use the criterion for classical motion from Landau and Lifshitz,[27] i.e.

$$\xi_{\text{classical}} = \frac{\mu \lambda\!\!\!^{-3} (-\frac{\partial V}{\partial R})}{\hbar^2} \ll 1 \qquad (48)$$

With one A.U. from the nucleus, $-\frac{\partial V}{\partial R} \leqslant 1$

$\therefore \xi_{\text{classical}} \leqslant 1$ around the neighborhood of the Bohr hydrogen atom.

From the above argument one sees that for the first threshold energy the incident electron follows a closely classical path; and only around the region of scattering does quantum phenomenon come into play. However, at higher energies and hence more hydrogenic states are energetically possible, then the classical $\int$-matrix ought to yield satisfactory results, with the possible exception at resonances,[10,28] comparable to quantum calculations.

APPENDIX A

Transformation Between Action-Angle Variables and Cartesian Coordinates

For reasons mentioned earlier, we want to specify the canonical coordinates[10] r, R, q_ℓ, q_j, q_J, qM_J and the related momenta p_r, p_R, ℓ, j, J, M_J (M_J denoting the projection of J on a particular axis), and to use these initial values to determine initial values for x, y, z, X, Y, Z, p_x, p_y, p_z, P_x, P_y, P_z, where the upper case letters refer to the relative Cartesian coordinates (momenta) between the electron and hydrogen atom, and the lower case represents the relative coordinates (momenta) between the bound electron and nucleus. $\underset{\sim}{R}$, $\underset{\sim}{r}$ can be transformed readily to the body-fixed Cartesian systems (q_1, q_2, q_3), (q_4, q_5, q_6), (q_7, q_8, q_9) that represent the three bodies. It is not hard to show the following:

$$
\begin{aligned}
s_i &= q_{i+6} - q_{i+3} \\
s_{i+3} &= q_i - (m_p q_{i+3} + m_e q_{i+6})/(m_p+m_e) \\
s_{i+6} &= \frac{1}{m_p+2m_e}(m_e q_i + m_p q_{i+3} + m_e q_{i+6})
\end{aligned}
\qquad \text{(A1)}
$$

where i = 1, 2, 3.

It is clear that $(s_1, s_2, s_3) = \underset{\sim}{r}$ and $(s_4, s_5, s_6) = \underset{\sim}{R}$ and (s_7, s_8, s_9) are the center of mass (CM) Cartesian coordinates of the whole system. A similar relationship between $P_j(j=1,2,\ldots,9)$ representing the momenta conjugate to the coordinates $(s_j, j=1,\ldots,9)$ and the momenta p_j, conjugate to the coordinates $q_j(j=1,\ldots,9)$ can be obtained via the point-contact transformation

$$
s_i = s_i(q_j) \quad \text{and so} \quad p_i = \sum_j P_j \left(\frac{\partial s_j}{\partial q_i}\right)
$$

They become

$$
\begin{aligned}
p_i &= P_{i+3} + \frac{m_e}{2m_e+m_p} P_{i+6} \\
p_{i+3} &= -P_i - \frac{[m_p]}{m_p+m_e} P_{i+3} + \frac{m_p}{m_p+2m_e} P_{i+6} \\
p_{i+6} &= P_i - \frac{m_e}{m_e+m_p} P_{i+3} + \frac{m_e}{2m_e+m_p} P_{i+6}
\end{aligned}
\qquad \text{(A2)}
$$

$$i = 1,2,3$$

In matrix notation

$$\underset{\approx}{p} = \underset{\approx}{A}\,\underset{\approx}{P} \quad \text{and} \quad \underset{\approx}{P} = \underset{\approx}{A}^{-1}\,\underset{\approx}{p}$$

Using the classical generator $F_3(Q,p)$ given by Whittaker,[17] the relationship between the action-angle variables and the Cartesian variables $\underset{\sim}{r} = (x,y,z)$ and $\underset{\sim}{p} = (p_x,p_y,p_z)$, $\underset{\sim}{R} = (X,Y,Z)$, $\underset{\sim}{P} = (P_x,P_y,P_z)$ are obtained through tedious algebraic inversion steps. The angle q_J may be set initially to any arbitrary value, qM_J is set to $\frac{\pi}{2}$ from the conservation of angular momentum.

With $\vec{r} = r\hat{r}$

$$
\begin{aligned}
\vec{p} &= p_r \hat{r} + \frac{j}{r}\hat{p}_1 \\
\vec{R} &= R\hat{R} \\
\vec{P} &= P_R\hat{R} + \frac{\ell}{R}\hat{P}_1
\end{aligned}
$$

then

$$
\hat{R} = \begin{pmatrix} \sin q_J \cos q_\ell + \lambda_1 \cos q_J \sin q_\ell \\ -\cos q_J \cos q_\ell + \lambda_1 \sin q_J \sin q_\ell \\ \sqrt{1-\lambda_1^2}\ \sin q_\ell \end{pmatrix} \qquad \text{(A3)}
$$

$$\hat{r} = \begin{pmatrix} -\sin q_J \cos q_j - \lambda_2 \cos q_J \sin q_j \\ \cos q_J \cos q_j - \lambda_2 \sin q_J \sin q_j \\ 1-\lambda_2^2 \sin q_j \end{pmatrix} \tag{A4}$$

$$\hat{P}_1 = \begin{pmatrix} -\sin q_J \sin q_\ell + \lambda_1 \cos q_J \cos q_\ell \\ \cos q_J \sin q_\ell + \lambda_1 \sin q_J \cos q_\ell \\ 1-\lambda_1^2 \cos q_\ell \end{pmatrix} \tag{A5}$$

$$\hat{p}_1 = \begin{pmatrix} \sin q_J \sin q_j - \lambda_2 \cos q_J \cos q_j \\ -\cos q_J \sin q_j - \lambda_2 \sin q_J \cos q_j \\ \cos q_j \ \ 1-\lambda_2^2 \end{pmatrix} \tag{A6}$$

where

$$\lambda_1 = (\ell^2-j^2+J^2)/2\ell J \tag{A7}$$

$$\lambda_2 = (j^2-\ell^2+J^2)/2jJ \tag{A8}$$

Now $\vec{j} = \vec{r} \times \vec{p}$ and $\vec{\ell} = \vec{R} \times \vec{P}$ we have furthermore:

$$\vec{j} = j \begin{pmatrix} 1-\lambda_2^2 \cos q_J \\ 1-\lambda_2^2 \sin q_J \\ \lambda_2 \end{pmatrix} \tag{A9}$$

$$\vec{\ell} = \ell \begin{pmatrix} -\ 1-\lambda_1^2 \cos q_J \\ -\ 1-\lambda_1^2 \sin q_J \\ \lambda_1 \end{pmatrix} \tag{A10}$$

$$\therefore \quad \vec{J} = \vec{\ell} + \vec{j} = \begin{pmatrix} 0 \\ 0 \\ J \end{pmatrix} \quad \text{for the proper helicity} \tag{A11}$$

APPENDIX B

Deflection Angle for Classical Trajectories

Here we shall give a method of obtaining the physically interesting quantity of classical scattering the deflection angle[2] Θ for the electron-hydrogen atom system. From classical mechanics, the deflection angle, for the collision of two particles subject to a central force, is given by:

$$\Theta = \pi - 2 \int_{r_<}^{\infty} dr\, r^{-2} \left[b^{-2} \ 1 - \frac{v(r)}{E} \ -r^{-2} \right]^{-\frac{1}{2}} \tag{B1}$$

where b is the impact parameter and $r_<$ is the classical turning point.

Consider the incident electron's direction as the Z axis, for proper helicity.[2] The initial body-fixed axes are designated as $\hat{X}$, $\hat{Y}$, and $\hat{Z}$.

Upon collision the emergent direction of the scattered electron is going to be different from the incident direction.

From the dynamics we can write down

$$\begin{pmatrix} X' \\ Y' \\ Z' \end{pmatrix} = \begin{pmatrix} a_{11} & a_{12} & a_{13} \\ a_{21} & a_{22} & a_{23} \\ a_{31} & a_{32} & a_{33} \end{pmatrix} \begin{pmatrix} X \\ Y \\ Z \end{pmatrix} \tag{B2}$$

or $\underset{\approx}{R}' = U_2 \underset{\approx}{R}$

Now it is possible to relate $Z' = a_{31}X + a_{32}Y + a_{33}Z$ from the values of the numerically integrated classical trajectories.

Next we can constrain X' to lie on the line of nodes so $a_{12} = 0$, this is equivalent to setting one of the Euler angles to zero.

Now we have the following five equations to solve:

$$a_{11}a_{31} + a_{13}a_{33} = 0$$

$$a_{21}a_{31} + a_{22}a_{32} + a_{23}a_{33} = 0 \qquad \text{orthogonality} \qquad \text{(B3)}$$

$$a_{11}a_{21} + a_{13}a_{23} = 0$$

$$a_{11}^2 + a_{13}^2 = 1$$

$$\text{normalization} \qquad \text{(B4)}$$

$$a_{21}^2 + a_{22}^2 + a_{23}^2 = 1$$

The result is

$$\underset{\approx}{U_2} = \begin{pmatrix} \frac{XZ}{R\sqrt{R^2-Z^2}} & \frac{YZ}{R\sqrt{R^2-Z^2}} & \frac{-\sqrt{R^2-Z^2}}{R} \\ \frac{-Y}{\sqrt{R^2-Z^2}} & \frac{X}{\sqrt{R^2-Z^2}} & 0 \\ \frac{X}{R} & \frac{Y}{R} & \frac{Z}{R} \end{pmatrix} \qquad \text{(B5)}$$

where $R = \sqrt{X^2 + Y^2 + Z^2}$.

This is the same result as that obtained by Pack and Hirschfelder.[29]

Here at this point it is of physical interest to note that an expression between the axes of the Bohr elliptical orbit and the $\underset{\approx}{R}$ and $\underset{\approx}{R}'$ vectors can be obtained.

From the action-angle variables before and after the collision process, the $\hat{x}$, $\hat{y}$, $\hat{z}$ axes of the elliptical orbit[15] can be written in of $\hat{X}$, $\hat{Y}$, $\hat{Z}$; z is chosen to be the normal of the elliptical plane of orbit in the right-hand screw convention.

Hence

$$\underset{\approx}{r} = \underset{\approx}{U_I} \underset{\approx}{R} \qquad \text{(B6)}$$

where U_I is a 3×3 matrix expressed in terms of action-angle variables and can be specified at either before or after the collision; U_I^i, U_I^f .

Since $\underset{\approx}{R}' = \underset{\approx}{U_2} \underset{\approx}{R}$, by means of a unitary transformation we have for the final elliptical-orbit coordinates, $\underset{\approx}{r}'$:

$$\underset{\approx}{r}' = \underset{\approx}{U_2}\, \underset{\approx}{U_I^f}\, \underset{\approx}{U_2}^{\dagger} \begin{pmatrix} X' \\ Y' \\ Z' \end{pmatrix} \qquad \text{(B7)}$$

$$\underset{\approx}{r}' = \begin{pmatrix} \xi \\ \eta \\ n \end{pmatrix} \qquad \text{(B8)}$$

where ξ refers to the minor axis

η refers to the major axis and points to the perihelion

n refers to the normal of the elliptical-plane and $\hat{n} = \hat{\eta}\times\hat{\xi}$

Using the notation for Euler angles from Goldstein[13] (pages 107-109) and the definition for the angle variables from Whittaker,[17] (pg. 349) we have then

$$\phi = \frac{\pi}{2} + q_J, \quad \theta = \cos^{-1}\left(\frac{jz}{j}\right), \quad \psi = \frac{\pi}{2} - q_j \qquad \text{(B9)}$$

$$\underset{\approx}{U}_I = \left(\begin{array}{c|c|c} -\sin q_j \sin q_J & \sin q_j \cos q_J & \sqrt{1-(\frac{jz}{j})^2}\cos q_j \\ -\frac{jz}{j}\cos q_J \cos q_j & +\frac{jz}{j}(-\sin q_J)\cos q_j & \\ \hline \cos q_j \sin q_J & -\cos q_j \cos q_J & \sqrt{1-(\frac{jz}{j})^2}\sin q_j \\ +\frac{jz}{j}\cos q_J \sin q_j & +\frac{jz}{j}(-\sin q_J)\sin q_j & \\ \hline \sqrt{1-(\frac{jz}{j})^2}\cos q_j & \sqrt{1-(\frac{jz}{j})^2}\sin q_j & \frac{jz}{j} \end{array}\right) \tag{B10}$$

Finally it may be instructive at this point to sketch the scheme for obtaining the deflection angle, using both the analytic solution for the initial (final) asymptotic distances and the numerically calculated trajectories. The sketch of an hypothetical trajectory is depicted in Fig. 2. The flowchart is as follows:

(1) An analytic form $r(\theta)$ is used from infinity to an appropriate distance, during which θ_1 is accumulated.

(2) The classical dynamics, with the appropriate semi-classical boundary conditions, i.e. action-angle variables, are followed by the Adams-Moulton[19] integrator routine, based on a predictor-corrector method.

(3) After obtaining via numerical means the proper final quantum conditions for the hydrogen atom, the analytic expression $r(\theta)$ is again employed from an appropriate cut-off distance out to infinity, where θ_2 is the deflection angle picked up for this region.

(4) $\mathfrak{L}'$, the final vectorial direction of the electron, is measured in the $\mathfrak{F}'$ system. In order to arrive at the actual deflection angle we must transform back to the original body-fixed axes system R

via the $\underset{\approx}{U}_2$ transformation so $\underset{\sim}{U}_2^{\dagger}\mathfrak{L}' = \underset{\sim}{\Phi}$ from which the deflection angle is readily obtainable.

APPENDIX C

Phase-Accumulation Consideration

Since the numerical integration and the asymptotic analytic solution are carried out in Cartesian coordinates (p,q) we must transform the phase of the S-matrix back to the action-angle variables (P,Q)[10] for the proper value of the phase.

From Goldstein[13] (pg. 241) the important relation is given, namely:

$$-\dot{Q}P = p\dot{q} = \frac{d}{dt}F_2(q,P) \tag{C1}$$

We then integrate from t_1 to t_2 to obtain:

$$\phi(P_2,P_1) = \phi(q_2,q_1) - F_2(q,P)\Big|_{t_1}^{t_2} \tag{C2}$$

where $\phi(q_2,q_1) = \int_{t_1}^{t_2} dt\, p\dot{q}$ and where $\vec{p}=(\vec{p},\vec{P})$, $\vec{q}=(\vec{r},\vec{R})$ (C3)

From Whittaker's[17] $F_3(p,Q)$ generator we integrate by parts and obtain for the direct (non-exchange) phase:

$$\phi_{P_2,P_1} = -\int_{t_0}^{t_3} dt(\underset{\sim}{R}\cdot\dot{\underset{\sim}{P}}) - \int_{t_1}^{t_2} dt\, \underset{\sim}{r}\cdot\dot{\underset{\sim}{p}}$$

$$+ (rp_r - f_2(r,n,j)\Big|_{t_1}^{t_2}$$

$$-[\ell q_\ell + JQ_J + \frac{\pi}{2}\,\frac{j^{*2}-\ell^2}{J}]\Big|_{t_0}^{t_3} \quad {}^{*}\text{evaluated at } t_1,t_2$$

$$-q_j j\Big|_{t_1}^{t_2} \tag{C4}$$

where t_0 is the starting time for the trajectory

t_1 is the start of the numerical integration

t_2 is the end of the integration

t_3 is the end of the trajectory.

$$f_2(r,n,j) = \left(2\left[\frac{-r^2}{2(n+j+1)^2} + r\right] - j^2\right)^{1/2} + (n+j+1)\left(\frac{\pi}{2} - \sin^{-1}\left(\frac{\left(1-\frac{r}{(n+j+1)^2}\right)}{\left(1-\frac{j^2}{(n+j+1)^2}\right)^{1/2}}\right)\right) - j\left(\frac{\pi}{2} + \tan^{-1}\left(\frac{r-j^2}{j\left(2\left(\frac{-r^2}{2(n+j+1)^2}+r\right)-j^2\right)^{1/2}}\right)\right) \tag{C5}$$

$f_2(r,n,j)$ can be given in closed form for a Coulomb potential, for more complicated ones, such as a Morse potential in three dimensions, one must evaluate $f_2(r,n,j)$ by numerical integration. It is worthwhile to note that, by virtue of our static dipole approximation the internal degrees of freedom of the hydrogen atom do <u>not</u> accumulate phase in the asymptotic regions.

The phase for exchange scattering is a little more complicated than that of the direct case because the final unperturbed Hamiltonian is of a different arrangement from the initial unperturbed Hamiltonian.

From the general rules of classical canonical transformation we have

$$\phi(P_2,P_1) = \phi(p_2,p_1) - F_4(p_2,P_2) + F_4(p_1,P_1) \tag{C6}$$

We shall designate a, b for the final and initial arrangements respectively. Making use of a $F_1[q^a(\bar{t})\ q^b(\bar{t})]$ generator, where $F_1(q^a(\bar{t}),\ q^b(\bar{t}))$ is a point transformation and $\bar{t}$ is the time of the

exchange, it can be shown that $\frac{d}{d\bar{t}}\ \phi(p_2{}^a,p_2{}^b) = 0$ so one can choose $\bar{t}=t_2$.

In this vein,

$$\phi(P_2{}^a,P_1{}^b) = F_2(q^b,P_1{}^b) - F_2(q_2{}^a,P_2{}^a) - \int_{t_1}^{\bar{t}} dt\ p^b q^b + \int_{\bar{t}}^{t_2} dt\ p^a \dot{q}^a \tag{C7}$$

can be now written as:

$$\phi(P_2{}^a,P_1{}^b) = \phi(p_2{}^a,p_2{}^b) - F_2(q_2{}^a,P_2{}^a) + F_2(q_1{}^b,P_1{}^b) + \sum p_2{}^a q_2{}^a - \sum p_1{}^b q_1{}^b \tag{C8}$$

Now in Eq. (C8)

$$F_2(q_2{}^a,P_2{}^a) = q^a_{\ell_2}\ell_2{}^a + q^a_{j_2} j_2{}^a + R_2{}^a P_2{}^a + f_2(r_2{}^a,n_2{}^a,j_2{}^a) \tag{C9}$$

and

$$\sum p_2{}^a q_2{}^a = q^a_{\ell_2}\ell_2{}^a + q^a_{j_2} j_2{}^a + R_2{}^a P_2{}^a + r_2{}^a p_2{}^a + J^a q_J{}^a + \frac{\pi}{2}\left(\frac{j_a{}^2-\ell_a{}^2}{J_a}\right). \tag{C10}$$

Likewise for $F_2(q_1{}^b,\ P_1{}^b)$ and $\Sigma p_2{}^b q_2{}^b$. At last collecting terms, we have the phase for exchange scattering:

$$\begin{aligned}\phi_{P_2{}^a,P_1{}^b} = &-\int_{t_0}^{t_2} dt(\underline{R}\cdot\dot{\underline{P}})_b - \int_{t_1}^{t_2} dt(\underline{r}\cdot\dot{\underline{p}})_b - \int_{t_2}^{t_3} dt(\underline{R}\cdot\dot{\underline{P}})_a \\ &+(f_2(r_1{}^b,n_1{}^b,j_1{}^b)-r_1{}^b p_1{}^b)\Big|^{t_1} \\ &-(f_2(r_2{}^a,n_2{}^a,j_2{}^a)-r_2{}^a p_2{}^a)\Big|^{t_2} \\ &-(\ell q_\ell + J q_J - \frac{\pi}{2}\ \frac{j^{2*}-\ell^2}{J})_a\Big|_{t_2}^{t_3} \qquad {}^*\text{evaluated at } t_2 \\ &-(\ell q_\ell + q_J J + \frac{\pi}{2}\frac{j^2-\ell^2}{J})_b\Big|_{t_0}^{t_2} - (jq_j)_b\Big|_{t_1}^{t_2}\end{aligned} \tag{C11}$$

ACKNOWLEDGEMENTS

First of all, I would like to express my gratitude to my research director, Professor William Miller, for his support and encouragement.

Fruitful discussions with C. C. Rankin, D. B. Coster, G. M. Denny, H. Arnett, R. D. Zimmerman and others were immensely enlightening to my graduate education at Berkeley.

Lastly, I thank my parents for their constant moral support.

All of the above work was done under the auspices of the Atomic Energy Commission through the Inorganic Materials Research Division of the Lawrence Radiation Laboratory at the University of California, Berkeley.

REFERENCES

1. Abrines, R. and Percival, I. C., Proc. Phys. Soc. (London) 88, 861 (1966); Burgess, A. and Percival I. C., Adv. Atom. Mol. Phys. 4, 109 (1968).
2. R. G. Newton, Scattering Theory of Waves and Particles, (McGraw-Hill Co., New York)(1966).
3. R. P. Feynman and A. R. Hibbs, Quantum Mechanics and Path Integrals (McGraw-Hill Co., New York), (1965).
4. Thomson, J. J., Phil. Mag. 23, 449; Rutherford, E. Phil. Mag. 21, 669.
5. P. G. Burke, A. J. Taylor, S. Ormonde, Proc. Phys. Soc. (London) 92, 345 (1967).
6. M. Gryzinski, Phys. Rev. 115, 374 (1959).
7. V. F. Brattsev and V. I. Ochkur, Soviet Phys. (JETP) 25, 631 (1967).
8. I. C. Percival and D. Richards, J. Phys. B: Atom. Molec. Phys. 3, 315-28 (1970); J. Phys. B 3, 1035 (1970).
9. W. H. Miller, J. Chem. Phys. 53, 1949 (1970).
10. W. H. Miller, J. Chem. Phys. 53, 3578 (1970).
    W. H. Miller, Chem. Phys. Let. 7, 431 (1970).
    W. H. Miller, J. Chem. Phys., "The Classical $\mathcal{J}$-Matrix for Rotational Excitation", (in press) (1971).
11. N. Wiener, Cybernetics (M.I.T.Press). (1964).
12. P. A. M. Dirac, Principles of Quantum Mechanics (Oxford U. P., New York, 1958), 4th edition, p. vii and p. 97.
13. H. Goldstein, Classical Mechanics (Addison-Wesley, Reading, Mass., 1950), pp. 288-307.
14. See, for example, A. B. Migdal and V. P. Krainov, Approximation Methods in Quantum Mechanics (W. A. Benjamin, Inc., New York, 1969),

p. 140 ff.

15. M. Born, The Mechanics of the Atom (Eng. Trans.)(Frederick Ungar Publishing Co., New York, 1960).

16. M. Karplus, R. N. Porter, R. D. Sharma, J. Chem. Phys. 43, 3259 (1965).

17. E. A. Whittaker, A Treatise on the Analytical Dynamics of Particles and Rigid Bodies, (Cambridge U.P., New York, 1960), pp. 348-351.

18. A. Messiah, Quantum Mechanics, Vol. II. (John Wiley & Sons, Inc., New York, 1962) p. 800.

19. E. Issacson, H. B. Keller, Analysis of Numerical Methods, (John Wiley & Sons, Inc., New York, 1966) pp. 384 to 400.

20. P. G. Burke, S. Ormonde, W. Whitaker, Proc. Phys. Soc. (London) 92, 319 (1966); Gailitis, M. K. and Damburg, R. Proc. Phys. Soc. 82, 192 (1963); Shelton, Baluja, Watson, J. Phys. B: Atom.Molec. Phys. 4, 71 (1971).

21. E. Merzbacher, Quantum Mechanics (John Wiley & Sons, Inc., New York) 2nd Edition, (1970).

22. S. Geltman, Topics in Atomic Collision Theory (Academic Press, New York, 1969), p. 106.

23. H. Bethe and E. Salpeter, Quantum Mechanics of One- and Two-Electron Atoms (Springer Verlag, New York, 1957), p. 229 ff.

24. L. Pauling and E. B. Wilson, Introduction to Quantum Mechanics (McGraw-Hill Co., New York, 1935) pp. 37 ff.

25. N. Mott and H. Massey, The Theory of Atomic Collisions (Oxford U. P., New York, 1949).

26. C. C. Rankin and W. H. Miller, J. Chem. Phys. (in press), 1971.

27. L. D. Landau and E. M. Lifshitz, Quantum Mechanics (Addison-

Wesley, Reading, Mass. 1958).

28. Recent work on the threshold behavior of the $H + H_2$ reaction shows that the tunneling formalism needs more refinement.

29. R. T. Pack and J. O. Hirschfelder, J. Chem. Phys. 49, 4409 (1968), Eq. (2.31).

TECHNICAL INFORMATION DIVISION
LAWRENCE RADIATION LABORATORY
UNIVERSITY OF CALIFORNIA
BERKELEY, CALIFORNIA 94720